Mutations in SARS-CoV-2 spike protein impair epitope-specific CD4$^+$ T cell recognition

Emily XC Tye[1], Elizabeth Jinks[1], Tracey A Haigh[1], Baksho Kaul[1], Prashant Patel[2], Helen M Parry[1], Maddy L Newby[3], Max Crispin[3], Nayandeep Kaur[1], Paul Moss[1], Samantha J Drennan[1], Graham S Taylor[1] and Heather M Long[1]

[1]Institute of Immunology and Immunotherapy, University of Birmingham, Edgbaston, Birmingham B15 2TT, UK

[2]Institute of Cancer and Genomics, University of Birmingham, Edgbaston, Birmingham B15 2TT, UK

[3]School of Biological Sciences, University of Southampton, Southampton, SO17 1BJ, UK

*Corresponding author: Dr Heather Long, Institute of Immunology and Immunotherapy, University of Birmingham, Edgbaston, Birmingham B15 2TT, UK

E-mail: h.m.long@bham.ac.uk

Tel: +44 (0) 121 414 6425

Running title: CD4$^+$ T cell responses to SARS-CoV-2 variants

Non-standard abbreviations: HCoV, human coronavirus; VOC, variant of concern; LCL, lymphoblastoid cell line; HCW, healthcare workers; PI, post-infection; PV, post vaccine

ABSTRACT

$CD4^+$ T cells are essential for protection against viruses, including SARS-CoV-2. The sensitivity of $CD4^+$ T cells to mutations in SARS-CoV-2 variants of concern (VOCs) is poorly understood. Here, we isolated 159 SARS-CoV-2-specific $CD4^+$ T cell clones from healthcare workers previously infected with wild-type SARS-CoV-2 (D614G) and defined 21 epitopes in spike, membrane and nucleoprotein. Lack of $CD4^+$ T cell cross-reactivity between SARS-CoV-2 and endemic beta-coronaviruses suggested these responses arose from naïve rather than pre-existing cross-reactive coronavirus-specific T cells. Ten of the 17 epitopes located in the spike protein were mutated in VOCs and $CD4^+$ T cell clone recognition of 7 of them was impaired, including 3 of the 4 epitopes mutated in omicron. Our results indicated that broad targeting of epitopes by $CD4^+$ T cells likely limits evasion by current VOCs. However, continued genomic surveillance is vital to identify new mutations able to evade $CD4^+$ T cell immunity.

INTRODUCTION

Coordinated adaptive immunity is essential for protection and clearance of viral infections, including SARS-CoV-2[1]. Virus-specific neutralising antibodies are considered the main correlate of protection against SARS-CoV-2 infection, but wane over time[2, 3]. T cell responses are more durable[2, 4, 5] and increasing evidence supports their role in restricting SARS-CoV-2 infection and limiting the severity of COVID-19[6, 7]. Worldwide efforts have rapidly delivered SARS-CoV-2 vaccines, mostly designed against the spike (S) protein, which mediates host cell entry. Studies enumerating the T cell response to whole SARS-CoV-2 S protein using pools of overlapping peptides covering the entire protein sequence (peptide mixes) show that memory T cell responses to S protein in previously-infected or vaccinated individuals are dominated by $CD4^+$ T cells[4, 8-10].

SARS-CoV-2 $CD4^+$ T cell epitopes have been identified, but mostly in assays that use high concentrations of stimulating peptides. In addition, their human leukocyte antigen (HLA) restriction has largely been inferred from *in silico* HLA-binding algorithms[11, 12]. Detailed knowledge of the specificity of $CD4^+$ T cell responses at the epitope level and their HLAII restriction is therefore currently lacking[13]. Furthermore, whether the $CD4^+$ T cell epitopes are naturally generated through the HLA class II (HLAII) antigen processing pathway is currently unknown. Because of these limitations, the extent to which $CD4^+$ T cells that recognise SARS-CoV-2epitopes cross-react with other human coronaviruses (HCoVs) remains unknown. Low frequency $CD4^+$ T cell reactivity to SARS-CoV-2 peptide mixes has been reported in some uninfected individuals[14-18] and has been suggested to originate from prior exposure to other HCoVs (HKU1, OC43, NL63, 229E, SARS or MERS). This raises the possibility that pre-existing HCoV immunity could potentially contribute to controlling SARS-CoV-2 infection.

The extent to which T cells induced by ancestral SARS-CoV-2 proteins can protect against variants of concern (VOCs) is a critical question. In particular, the highly-transmissible omicron VOC contains several mutations within the receptor binding domain (RBD) of S protein, the main target of

neutralising antibodies[19, 20]. These mutations reduce neutralisation by the S-specific antibodies induced by ancestral SARS-CoV-2 variants or by the initial vaccines deployed in the pandemic, which were designed against the original S protein reference sequence[21-23]. Whilst neutralising antibody titres can be partially restored by booster vaccination[24, 25], continued virus evolution has caused a high prevalence of secondary and vaccine breakthrough infections[26]. *Ex vivo* studies of previously infected or vaccinated individuals using peptide mixes have shown minimal reduction in the overall frequency of $CD4^+$ T cell responses against the alpha (B.1.1.7), beta (B1.351), gamma (P1) and delta (B.1.717.2)[23, 27-29] or omicron (B.1.1.529) VOCs[22, 30, 31]. However, biologically relevant differences in epitope-specific recognition efficiency may have been missed[32] and little information exists to understand the extent of $CD4^+$ T cell epitopes evaded by current VOCs or to predict $CD4^+$ T cell epitope loss in future SARS-CoV-2 variants.

Here, we performed a detailed analysis of $CD4^+$ T cell immunity against SARS-CoV-2 in healthcare workers (HCW) infected in the first wave of the pandemic. We examined 159 $CD4^+$ T cell clones and identified and characterised 21 HLAII-restricted T cell epitopes. Responses to most epitopes located in the S protein were also present in vaccinated individuals of appropriate HLAII genotype. Cross-reactivity of SARS-CoV-2 S-specific T cell clones was only observed against the closely related S2 region of the SARS virus, with no cross-reactivity observed for any other β-HCoV. Mutations were present in 10 of the 17 S protein epitopes within one or more SARS-CoV-2 VOC. Minor amino acid (aa) changes in 7 epitope sequences, including those within the RBD region of omicron, were sufficient to reduce or evade recognition by S-specific $CD4^+$ T cells. However, the breadth of responses to multiple $CD4^+$ T cell epitopes seen in each individual suggested that current VOC mutations confer only limited evasion from $CD4^+$ T cell surveillance.

RESULTS

SARS-CoV-2 infection induces broad CD4$^+$ T cell immunity

Peripheral blood mononuclear cells (PBMCs) were collected in June-September 2020 from 20 HCW 3-6 months post infection (PI) during the first wave of SARS-CoV-2 wild-type (WT,D614G) infection in the UK and 14 uninfected healthy (UH) volunteers. HCW-PI had detectable antibodies to S protein and nucleoprotein (N) at this timepoint, while UH volunteers had no detectable S or N-specific antibody responses (Extended Data Fig. 1). To characterise T cell immunity against whole antigens, PBMCs and CD8-depleted PBMCs (hereafter CD8$^-$PBMCs) were tested against SARS-CoV-2 peptide mixes comprising 15mer peptides overlapping by 11aa and spanning the entire open reading frame of S, membrane (M) and N proteins in *ex vivo* interferon-γ (IFN-γ) Elispot assays. Compared to control whole PBMCs, as expected, the response to a peptide mix of HLA class I (HLAI)-restricted epitopes was significantly lower in CD8$^-$PBMCs (Fig. 1a, b). In contrast, responses to S protein (tested as two pools, S1 and S2), M and N peptide mixes were increased in CD8$^-$PBMCs (Fig. 1a, b), confirming CD4$^+$ T cell memory responses were predominant [4, 8]. As previously reported[14-18], we detected weak responses to individual SARS-CoV-2 proteins in CD8$^-$PBMCs from 8 of 14 UH volunteers (Fig. 1c). The magnitude of responses in UH volunteers was significantly lower than in HCW-PI (P<0.01, two-sided Mann-Whitney U test) (Fig. 1c) and may represent cross-reactive T cells primed by prior exposure to β-HCoVs.

We next examined the CD4$^+$ T cell response to S, M and N proteins following SARS-CoV-2 infection at the epitope level. Polyclonal CD4$^+$ T cell lines were initially established from HCW-PI by stimulating PBMCs with S, M and N peptide mixes, ensuring complete coverage of the proteins. These lines were then tested with individual 20mer peptides overlapping by 10aa, or DMSO solvent as negative control, to determine the regions of reactivity against each protein. CD4$^+$ T cells can be expanded

using shorter 15mer peptides, however the optimal response is often to a longer peptide[33, 34]. For each individual, the polyclonal CD4+ T cell lines contained multiple responses against peptides distributed throughout the S protein, including the RBD, S1 and S2 regions, M and N (Fig. 1d). As noted by others, these data show that SARS-CoV-2 induced a broad CD4+ T cell response[11, 14].

HLAII type determines SARS-CoV-2 CD4+ T cell epitope responses

We next performed limiting dilution cloning from 5 individuals with different HLAII types and isolated CD4+ T cell clones specific for 21 epitopes (17 S protein, 2 M protein and 2 N protein epitopes). To identify the optimal peptide recognised by each T cell clone, we titrated four individual 20mer peptides (overlapping by 15aa) covering the regions where T cell reactivity was detected in the screening assays. This defined peptides SSAN (aa 161-180) and FNCY (aa 486-505) as the epitopes for the CD4+ T cell clones c3 and c42, respectively (Fig. 2a). Peptides RGHL and RNSS were defined using the same approach in M and N respectively (Extended Data Fig. 2). The avidities of the S, M and N specific T cell clones were comparable to CD4+ T cell clones against other viruses previously measured by peptide titration (Fig.2 and Extended Data Fig. 2)[35-37].

Next, to identify the HLAII allele restricting each epitope we tested each clone against a peptide-loaded autologous lymphoblastoid cell line (LCL) in the presence of blocking antibodies against HLA-DR, HLA-DP and HLA-DQ, and after that against peptide-loaded allogeneic LCLs with partially matched HLA-DR, -DP or -DQ types. This approach indicated that HLA-DPB1*04:01 restricted the presentation of peptide SSAN to clone c3, while HLA-DRB1*01:01 presented peptide FNCY to clone c42 (Fig. 2b, c). We then defined the optimal peptide and presenting HLAII allele for all 21 S, M and N epitopes (Table 1), using the clones isolated against each epitope (Supplementary Table 1). Individual T cell clones specific for the same epitope recognised the same optimal peptide and HLAII combination (Extended Data Fig. 3). The T cell clones specific for all 17 S protein epitopes recognised

autologous LCL pre-exposed to low concentrations of purified S protein (1ng/ml) (Fig. 2d and Extended Data Fig. 4), indicating that all S protein epitopes were efficiently generated through the exogenous HLAII processing pathway. All 21 S, M and N epitopes were presented by HLA-DR or HLA-DP alleles, with no HLA-DQ-restricted T cells found (Table 1).

To address if natural infection and vaccination elicited similar $CD4^+$ T cell immunity, we repeated the *ex vivo* Elispots assays for the production of IFN-γ by $CD8^-$PBMCs from each HCW-PI using the defined epitope peptides appropriate to each individual's HLAII type. Of the eleven epitopes presented by HLAII alleles present in multiple donors, responses to 9 were present in more than one donor (Table 1). Next, we examined the relative immunogenicity of SARS-CoV-2 vaccination by testing blood samples collected 1-5 months post-vaccine from 9 of the 14 donors originally used as UH. All 9 donors had S-specific antibodies, but undetectable N-specific antibodies (Extended Data Fig. 5), indicating they had responded to vaccination and had no history of natural infection. Based on the HLAII genotypes of these donors, we tested 14 S epitopes and detected responses to 13 in *ex vivo* IFNγ Elispot assays (Table 1). Collectively, these results indicated that SARS-CoV-2 infection and vaccination induced broad $CD4^+$ T cell responses to shared epitopes and that in both contexts HLAII genotype was a key determinant of the SARS-CoV-2 S-specific $CD4^+$ T cell response.

Spike-specific $CD4^+$ T cell clones do not cross-recognise β-HCoVs

Next we asked whether spike-specific $CD4^+$ T cells elicited by SARS-COV-2 infection cross reacted with closely related β-HCoVs known to infect humans (SARS, MERS, HKU1 and OC43), in which the S proteins share 34-76% aa similarity to SARS-CoV-2 S protein (Fig. 3a). Within the N-terminal S1 region, the highest similarity (64.7%) is between SARS and SARS-CoV-2, whilst the similarity of all other β-HCoV S1 regions with SARS-CoV-2 S1 is low (<32%) (Fig. 3b). The C-terminal S2 regions exhibit greater overall similarity, with SARS-CoV-2 and SARS having 90.0% similarity, and the similarity between SARS-CoV-2 and the other β-HCoV is up to 45%[38] (Fig. 3b).

$CD4^+$ T cell clones specific for 6 SARS-CoV-2 S epitopes were tested against peptide mixes comprising 15mer peptides overlapping by 11aa from each β-HCoV or DMSO solvent as a negative control. As expected, all 6 S protein-specific clones showed similar recognition against S1 or S2 SARS-CoV-2 peptide mix and the clone's respective cognate epitope peptide (Fig. 3c, d). The SSAN c3, VVLS c21 and FNCY c42 T cell clones specific for epitopes located within the more divergent S1 region of SARS-CoV-2 did not cross-recognise any other β-HCoV peptide mix (Fig 3c). These SARS-CoV-2 20mer epitopes had between 2 and 8 aa differences compared to the corresponding regions of SARS (Fig. 3c), the virus with greatest overall sequence similarity (Fig. 3a); the corresponding epitope sequences within the other β-HCoVs were even more divergent (Fig. 3c). Of the $CD4^+$ T cell clones specific for three epitopes within the S2 region of SARS-CoV-2, which has greater aa similarity with other β-HCoVs (Fig. 3b), NFSQ c117 did not cross recognise any other β-HCoV (Fig. 3d). STEC c41 and SFIE c55 both cross-recognised the SARS peptide mix, but not the MERS, HKU1 or OC43 peptide mixes (Fig. 3d); both epitopes had only a single aa difference between SARS-CoV-2 and SARS (Fig. 3d). We extended the work to an additional 11 clones, 5 specific for epitopes within S1 and 6 within S2. The epitopes within the S1 region of SARS-CoV-2 differed from SARS by 5-16 aa, whereas the epitopes within the S2 region differed by 0-2 aa (Extended data Fig. 6). None of the 5 S1-specific clones, but all 6 S2-specific clones, cross-recognised the SARS peptide mix (Table 2); the peptide mixes from the other β-HCoVs, with lower aa sequence similarity to SARS-CoV-2, were never recognised (Table 2). These data indicated that S epitope-specific $CD4^+$ T cells isolated following SARS-CoV-2 infection could recognise highly homologous epitopes within the S2 region of SARS, but did not cross-react with MERS or the extant β-HCoVs HKU1 and OC43, consistent with the S protein-specific $CD4^+$ T cell clones described here being primed by SARS-CoV-2 infection.

Mutations in variants of concern impair CD4$^+$ T cell recognition

Next we examined the recognition of previous and current SARS-CoV-2 VOCs, including alpha (B.1.1.7), beta (B.1.351), gamma (P.1), delta (B.1.617.2), zeta (P.2), theta (P.3) and omicron BA.1 and BA.2 (B.1.1.529), by S protein-specific CD4$^+$ T cell clones. Amino acid substitutions or deletions were present in 10 of the 17 S epitope sequences within VOCs (Table 3), with some common to multiple VOCs, such as the N501Y mutation in the FNCY epitope identified in alpha, beta and gamma variants (Table 3), and others unique to particular viral isolates, such as the N764K mutation within the STEC epitope in omicron (Table 3). To study the impact of these mutations on CD4$^+$ T cell recognition, we tested the S-specific CD4$^+$ T cell clones from the HCW-PI donors, who had been infected during the WT (D614G) wave of SARS-CoV-2, against the optimal WT epitope peptide and the corresponding mutated peptides from the VOCs. 20mer peptides were employed to encompass the peptide flanking regions, as mutations within the MHCII-binding core and proximal flanking regions can interfere with epitope binding to MHCII[39]. Peptides were tested at concentrations of 10^{-5} to 10^{-11}M to detect effects of these mutations at low concentrations that may not be evident at higher concentrations. Single central aa substitutions in epitope TLVK (N969K) in omicron and SGTN (D80Y) in zeta eliminated CD4$^+$ T cell recognition, except at supra-physiological peptide concentrations for the latter (Fig. 4). Two separate point mutations in epitope QLIR, A1022S in beta and T1027I in gamma impaired CD4$^+$ T cell recognition at equivalent peptide concentrations (Fig. 4). However, several epitope peptides containing point mutations, such as LSET (T307A) in theta, STEC (N764K) in omicron and TYVT (A1022S) in beta were recognised equally to the WT epitope (Fig. 4). A double aa deletion (Δ43-44) in theta had no effect on the recognition of LVDL and TRFQ epitopes (Fig. 4); however, a triple aa deletion (Δ42-44) in beta reduced CD4$^+$ T cell stimulation compared to the WT peptide (Fig. 4).

The epitopes with most mutations were GGNY and FNCY, both present within the RBD region, a frequent target of mutation in VOCs[19, 20]. Although single point mutations arising in earlier VOCs in

epitopes GGNY (L452R in delta and B.1.324) and FNCY (N501Y in alpha, beta, gamma and theta) did not affect recognition, the multiple mutations accumulated in omicron in GGNY (G446S, L452R, R457N) and FNCY (Q493K, G496S, Q498R, N501Y, Y505H) eliminated recognition by the $CD4^+$ T cells specific for these epitopes (Fig. 4). Overall, recognition of 7 of the 17 epitopes in S protein by the $CD4^+$ T cells specific for these epitopes was affected by mutations present in one or more VOCs (Fig. 4, Table 3). The affected epitopes were restricted through a range of HLAII alleles (Table 1), and in every case where recognition of an epitope was lost, the same person possessed $CD4^+$ T cell responses against other epitopes that were not impacted by mutation (Fig. 1d).

T cell clones only allow a small number of TCRs to be studied. *In vivo*, epitope-specific $CD4^+$ T cell responses comprise a multitude of different TCRs[40]. To test whether other TCRs specific for the same epitopes may be unaffected by VOC mutations, we examined *ex vivo* memory $CD4^+$ T cell ($CD4^+$ T_M cells) populations specific for S protein epitopes in HCW-PI or in UH 1-5 months post-vaccination. First, to analyse the clonal TCR composition of the SARS-CoV-2 infection-induced $CD4^+$ T_M cells specific for S protein epitopes we used three representative peptide-HLAII (pHLAII) tetramers (Tet) containing epitope sequences from the WT S protein: one epitope that contained no mutations in the current VOCs, SSAN (DPB1*04:01/SSAN), one epitope where mutation in the omicron VOC abrogated T cell clone recognition, GGNY (DPB1*02:01/GGNY) and one where the current VOC mutations did not affect T cell clone recognition, STEC (DRB1*15:01/STEC) (Extended data Fig. 7a, b). The pHLAII Tet were used in flow cytometry assays alongside a panel of antibodies specific for 21 TCR Vβ segments commonly expressed on $CD4^+$ T cells[41]. As expected, in every case, the S epitope-specific $CD4^+$ T_M cells were polyclonal, with evidence of oligoclonal expansion (Fig. 5a and Extended data Fig. 7c). Several TCR Vβ segments were over-represented within the pHLAII Tet^+ $CD4^+$ T_M cells compared to the total $CD4^+$ T_M cell repertoire, with smaller frequencies of pHLAII Tet^+ $CD4^+$ T_M cells expressing other TCR Vβs also detected (Fig. 5a).

Second, we performed IFN-γ Elispot assays using $CD8^-$PBMCs from HCW-PI or UH 1-5 months post-vaccine to test the response of $CD4^+$ T_M cells to 5 epitopes, 4 of which (SGTN, LVDL, GGNY and QLIR) had shown decreased $CD4^+$ T cell clone recognition against VOC peptides and one, STEC, that had maintained recognition. Compared to the WT peptide, the frequency of $CD4^+$ T cells that produced IFN-γ in response to the zeta SGTN peptide containing the point mutation (D80Y) was lower at each peptide concentration tested (Fig. 5b). Likewise, the recognition of LVDL, GGNY and QLIR similarly showed reduced T cell responses for at least one of the variant peptides tested. Notably, no ex vivo IFN-γ Elispot response was detected to the mutated GGNY omicron peptide (G446S, L452R, R457N) (Fig. 5b) in the same individual that possessed a polyclonal population of pHLAII Tet^+ cells specific for the WT peptide (Fig. 5a). In contrast, similar magnitudes of IFN-γ producing $CD4^+$ T cells were detected against the STEC peptide in omicron (N764K) and WT (Fig. 5b). Collectively these data showed the acute sensitivity of SARS-CoV-2 S-specific $CD4^+$ T cells to small aa changes in their epitope sequence and that our findings using T cell clones were representative of circulating polyclonal epitope-specific $CD4^+$ T cell responses.

DISCUSSION

Our detailed analysis of HCW previously infected with wild-type SARS-CoV-2, including the isolation and extensive use of $CD4^+$ T cell clones, provided several new insights into the $CD4^+$ T cell response to SARS-CoV-2. Focusing on the S protein, the lack of cross-reactivity with HCoVs indicated that all the SARS-CoV-2 S-specific $CD4^+$ T cell clones originated from the naïve repertoire rather than pre-exisiting HCoV-specific $CD4^+$ T_M cells. A key finding was that the $CD4^+$ T cell response in every individual targeted multiple viral epitopes. This broad response is important because we showed mutations in SARS-CoV-2 VOCs compromise $CD4^+$ T cell recognition of some, but currently not all, S epitopes. The breadth of the $CD4^+$ T cell response therefore limits the impact of mutations in current VOCs on overall $CD4^+$ T cell surveillance.

In line with previous studies on HCW-PI assessing T cell responses to whole antigens *ex vivo*[4, 8-10], we detected robust $CD4^+$ T_M cell responses against peptide mixes from SARS-CoV-2 S, M and N proteins. Our data showed that every donor possessed a broad $CD4^+$ T cell response after SARS-CoV-2 infection, which targeted multiple epitopes. In total, we defined 21 HLAII-restricted epitopes. This considerably expanded the number of experimentally verified $CD4^+$ T cell epitopes and also specified the HLAII restriction of some previously reported epitopes[11-13, 42, 43]. Some of our epitopes were presented by HLAII alleles found at high frequency in global populations, such as the HLA-DRB1*04 subtypes, DRB1*01:01, DRB1*15:01 and DPB1*04:01[44]. $CD4^+$ T cell responses to these epitopes are therefore likely to be widespread following infection or vaccination. Our data considerably strengthens the evidence that SARS-CoV-2 epitopes are skewed towards HLA-DP and HLA-DR restriction alleles[14, 25]. This HLAII usage is distinct from other human viruses investigated using $CD4^+$ T cell clones[37, 45].The reason remains unclear, but it will be important to understand, as our data showed that HLAII genotype was a key determinant of the $CD4^+$ T cell response to S protein following either SARS-CoV-2 infection or vaccination.

Several endemic HCoVs infect humans and cause mild disease. T cells elicited by prior infection with these viruses could modulate the course of disease, if they cross-reacted with SARS-CoV-2. All the $CD4^+$ T cell clones we studied were generated using SARS-CoV-2 peptides from donors previously infected with SARS-CoV-2, who also had evidence of historical infection with the extant β-HCoVs HKU1 and OC43. All S protein-specific $CD4^+$ T cell clones efficiently recognised SARS-CoV-2 S protein peptide mix, but not the peptide mixes from OC43 or HKU1 S proteins, which have <40% aa similarity to SARS-CoV-2. The only observed cross-reactivity to β-HCoV was against epitopes located within the S2 region of SARS, which has 90% aa similarity with SARS-CoV-2, but to which the UK HCWs studied here had never been exposed. These results strongly suggested that, for our cohort of previously SARS-CoV-2 infected donors, $CD4^+$ T cell clones specific for the S protein originated from naïve $CD4^+$ T cells primed by SARS-CoV-2 infection rather than from $CD4^+$ T_M cells primed by prior HCoV infections. Consistent with our data, $CD8^+$ T_M cells specific for an epitope in the SARS-CoV-2 N protein originated from the naïve $CD8^+$ T cell repertoire in SARS-CoV-2 infected individuals[46].

Our data do not contradict previous studies that have reported the presence of pre-existing cross-reactive S-specific $CD4^+$ T cells in unexposed individuals[14-17]. Where cross-reactivity has been investigated at the level of epitopes, it was focused on small regions of the S protein that are highly conserved between SARS-CoV-2 and other HCoVs[13-15, 18, 47] Our data showed that following SARS-CoV-2 infection, the $CD4^+$ T cell response to the S protein was broadly targeted across the entire protein. Therefore, most $CD4^+$ T_M cell responses to SARS-CoV-2 S protein targeted epitopes with low sequence similarity to other HCoVs S protein and, as expected, did not cross-react.

We only investigated the cross-reactivity of $CD4^+$ T cells specific for the S protein, which is highly targeted by mutation. Other viral proteins are more conserved across HCoVs and T cell cross-reactivity may therefore be more likely. Accordingly, pre-existing T cell immunity against the highly conserved N and ORF1ab-encoded NSP proteins has been reported in SARS-CoV-2-exposed HCWs with no evidence of virus infection[15, 16, 48]. The HCoV cross-reactive T cells in those donors were

frequently directed against epitopes located in the early-expressed replication transcription complex encompassing Nsp7, Nsp12 and NSp13[48]. Ultimately, the extent to which pre-existing cross-reactive T cell immunity contributes to controlling SARS-CoV-2 infection in an individual might be determined by a complex combination of factors, including the conservation of the epitopes presented by their HLA genotype, their TCR repertoire and their history of previous HCoV exposure[13].

Examining S proteins sequences from VOCs, we identified aa substitutions or deletions in 10 of the 17 S protein $CD4^+$ T cell epitopes; some were common to multiple VOCs, while others were unique to particular viral isolates. Combining data from the $CD4^+$ T cell clone experiments and the experiments using ex vivo PBMCs, which contain polyclonal epitope-specific populations, we found variable effects of the epitope mutations on $CD4^+$ T cell recognition. Triple aa deletion and multiple aa substitutions within individual epitopes had the greatest impact on $CD4^+$ T cell recognition[49]. The effect of point mutations was complex. A single mutation could markedly decrease $CD4^+$ T cell recognition or have no effect. Notably, decreased $CD4^+$ T cell sensitivity to several epitopes was only apparent at lower peptide concentrations and was not evident using the high concentrations of peptides previously employed[22, 23, 29, 50]. This highlights the requirement for further careful experimental definition of the currently known immunodominant SARS-CoV-2 $CD4^+$ T cell epitopes, the identification of the essential aa required for HLAII binding and TCR engagement and the need to consider each epitope individually. The epitope mapping presented here provides a rational basis for VOC risk stratification. Additional mutations recently acquired in the BA.4 and BA.5 omicron variants, such as Δ69-70 and F486V highlight the continued evolution of SARS-CoV-2 and potential for further T cell epitope mutation.

In conclusion, our study demonstrated the fine sensitivity of SARS-CoV-2 S-specific $CD4^+$ T cells to aa variation in epitope sequence and the potential for SARS-CoV-2 evolution to evade the $CD4^+$ T_M response. The breadth of SARS-CoV-2 S epitopes targeted in every individual indicated current VOC mutations are likely to have only limited impact on overall $CD4^+$ T cell surveillance. However,

continued evolution of SARS-CoV-2 could lead to further epitope loss and continued monitoring of emerging VOCs is important.

ACKNOWLEDGEMENTS

This work was supported by the UK Coronavirus Immunology Consortium (UK-CIC) funded by NIHR/MRC MR/V028448/1. We acknowledge support from the International AIDS Vaccine Initiative (IAVI) through Grant INV-008352/OPP1153692 funded by the Bill and Melinda Gates Foundation and the University of Southampton Coronavirus Response Fund (MC). The authors would like to acknowledge the Flow Cytometry Platform at the University of Birmingham.

AUTHOR CONTRIBUTIONS

HL designed and supervised the study. ET, EJ, TH, BK, NK, SD and HL performed *in vitro* assays. ET, EJ, TH, BK, NK, SD, PM, GT and HL perfomed data analysis. PP and HP conducted sample collection. MN and MC generated and provided essential reagents. GT and HL led on data interpretation and wrote the paper. All authors commented on the manuscript.

COMPETING INTERESTS STATEMENT

The authors declare no competing interests

Table 1 – SARS-CoV-2 CD4+ T-cell epitopes and responses

Protein	aa coordinates	Epitope	HLA II restriction	HCW-PI	UH-PV
Spike	71-90	SGTNGTKRFDNPVLPFNDGV	DPB1*05:01	2/2	NT
Spike	161-180	SSANNCTFEYVSQPFLMDLE	DPB1*04:01	2/2	1/2
Spike	226-245	LVDLPIGINITRFQTLLALH	DRB1*04:01, *04:03, *04:04	1/1	1/2
Spike	236-255	TRFQTLLALHRSYLTPGDSS	DRB1*04:02	1/1	0/1
Spike	296-315	LSETKCTLKSFTVEKGIYQT	DRB1*04:01, *04:04	1/2	2/2
Spike	446-465	GGNYNYLYRLFRKSNLKPFE	DPB1*02:01	3/3	1/2
Spike	486-505	FNCYFPLQSYGFQPTNGVGY	DRB1*01:01	2/4	1/2
Spike	511-530	VVLSFELLHAPATVCGPKKS	DRB1*01:01	3/4	2/3
Spike	746-765	STECSNLLLQYGSFCTQLNR	DRB1*15:01	2/2	5/5
Spike	801-820	NFSQILPDPSKPSKRSFIED	DRB1*04:01, *04:03, *04:04	2/2	2/2
Spike	816-835	SFIEDLLFNKVTLADAGFIK	DRB1*08:01	1/1	2/2
Spike	891-910	GAALQIPFAMQMAYRFNGIG	DRB1*07:01	3/5	2/3
Spike	956-975	AQALNTLVKQLSSNFGAISS	DRB1*01:01	2/4	2/3
Spike	961-980	TLVKQLSSNFGAISSVLNDI	DRB1*04:01, *04:04	1/1	2/2
Spike	1006-1025	TYVTQQLIRAAEIRASANLA	DRB1*04:02	1/1	NT
Spike	1011-1030	QLIRAAEIRASANLAATKMS	DRB1*04:01, *04:04	1/2	1/2
Spike	1061-1080	VFLHVTYVPAQEKNFTTAPA	DRB1*04:02	1/1	NT
Membrane	146-165	RGHLRIAGHHLGRCDIKDLP	DRB4*01:03	NT	N/A
Membrane	161-180	IKDLPKEITVATSRTLSYYK	DRB1*04:02	NT	N/A
Nucleoprotein	196-215	RNSSRNSTPGSSRGTSPARM	DPB1*09:01	NT	N/A
Nucleoprotein	281-300	QTQGNFGDQELIRQGTDYKH	DRB4*01:03	NT	N/A

HCW-PI – healthcare workers post infection; UH-PV – uninfected healthy individuals post vaccine.

Table 2 – CD4+ T cell clone recognition of β-HCoV peptide mixes

Spike Region	aa coordinates	Epitope	SARS-CoV-2	SARS	MERS	HKU1	OC43
S1	71-90	SGTN	+	-	-	-	-
	161-180	SSAN	+	-	-	-	-
	226-245	LVDL	+	-	-	-	-
	236-255	TRFQ	+	-	-	-	-
	296-315	LSET	+	-	-	-	-
	446-465	GGNY	+	-	-	-	-
	486-505	FNCY	+	-	-	-	-
	511-530	VVLS	+	-	-	-	-
S2	746-765	STEC	+	+	-	-	-
	801-820	NFSQ	+	-	-	-	-
	816-835	SFIE	+	+	-	-	-
	891-910	GAAL	+	+	-	-	-
	956-975	AQAL	+	+	-	-	-
	961-980	TLVK	+	+	-	-	-
	1006-1025	TYVT	+	+	-	-	-
	1011-1030	QLIR	+	+	-	-	-
	1061-1080	VFLH	+	+	-	-	-

Table 3 – S epitope sequences in SARS-CoV-2 WT and VOCs

aa coordinates	Epitope sequence	Pango lineage	T cell Recognition
71-90 SGTN	SGTNGTKRFDNPVLPFNDGV	WT	+++
	SGTNGTKRF**Y**NPVLPFNDGV	Zeta	-
226-245 LVDL	LVDLPIGINITRFQTLLALH	WT	+++
	LVDLPIGINITRFQTLL$^{\Delta\Delta}$ HRS	Theta	+++
	LVDLPIGINITRFQTL $^{\Delta\Delta\Delta}$HRSY	Beta	+
236-255 TRFQ	TRFQTLLALHRSYLTPGDSS	WT	+++
	TRFQTLL$^{\Delta\Delta}$ HRSYLTPGDSSSG	Theta	+++
	TRFQTL $^{\Delta\Delta\Delta}$HRSYLTPGDSSSGW	Beta	++
	TRFQTLLALHRSYLTPGDS**F**	A23.1	+++
296-315 LSET	LSETKCTLKSFTVEKGIYQT	WT	+++
	LSETKCTLKSF**A**VEKGIYQT	Theta	+++
446-465 GGNY	GGNYNYLYRLFRKSNLKPFE	WT	+++
	GGNYNY**R**YRLFRKSNLKPFE	Delta, B.1.324	+++
	SGNYNY**R**YRLF**N**KSNLKPFE	Omicron	-
486-505 FNCY	FNCYFPLQSYGFQPTNGVGY	WT	+++
	FNCYFPLQSYGFQPT**Y**GVGY	Alpha, beta, gamma, theta	+++
	FNCYFPL**K**SY**S**F**R**PT**Y**GVG**H**	Omicron	-
746-765 STEC	STECSNLLLQYGSFCTQLNR	WT	+++
	STECSNLLLQYGSFCTQL**K**R	Omicron	+++
961-975 TLVK	TLVKQLSSNFGAISS	WT	+++
	TLVKQLSS**K**FGAISS	Omicron	-
1006-1025 TYVT	TYVTQQLIRAAEIRASANLA	WT	+++
	TYVTQQLIRAAEIRAS**S**NLA	Beta	+++
1011-1030 QLIR	QLIRAAEIRASANLAATKMS	WT	+++
	QLIRAAEIRAS**S**NLAATKMS	Beta	++
	QLIRAAEIRASANLAA**I**KMS	Gamma	++

T cell recognition was quantified as the fold increase in concentration required to yield T cell activity equivalent to the EC50 of the WT peptide. +++ equivalent concentration, ++ 1-2 log increased peptide, and + 3 log increased peptide. - no T cell response detected.

FIGURE LEGENDS

Figure 1. CD4$^+$ T cell response to SARS-CoV-2. (a) Representative Elispot assays for the production on IFN-γ in whole and CD8-depleted PBMCs (CD8$^-$PBMCs) isolated from HCW-PI, plated at 2x10^5 cells/well and incubated with mixes of 15aa peptides (overlapping by 11aa) from SARS-CoV-2 S1, S2, M and N proteins, control HLAI and HLAII epitope mixes and DMSO solvent (Neg). (b) Summary of Elispot assays for the production of IFN-γ in whole versus CD8$^-$PBMCs using n=10 HCW-PI incubated with peptide mixes as in a. Results are shown as mean spot forming cells (SFC) per 10^6 PBMCs. Significance was determined by two-sided Wilcoxon test *p<0.05. (c) Summary of Elispot assays for the production of IFN-γ in CD8$^-$PBMCs from HCW-PI (n=20) and UH (n=14) individuals incubated with peptide mixes as in a. Results are shown as mean spot forming cells (SFC) per 10^6 CD8$^-$PBMCs. Significance was determined by two-sided Mann-Whitney U test **p<0.01. (d) Summary of ELISAs measuring IFN-γ production by polyclonal CD4$^+$ T cell lines generated by initial stimulation of CD8$^-$PBMCs with peptide mixes as in a, then stimulated 7-14 days later with individual 20mer peptides (overlapping by 10aa) spanning the relevant SARS-CoV-2 protein. Individual rows show the response from HCW-PI, n=11.

Figure 2. Characterisation of novel spike CD4$^+$ T cell epitopes. (a) ELISA assays for the production of IFN-γ from CD4$^+$ T cell clones cocultured in overnight assays with autologous lymphoblastoid cell line (LCL) loaded with individual 20mer peptides overlapping by 15aa (10^{-5} to 10^{-11}M). (b-d) ELISA assays for the production of IFN-γ from CD4$^+$ T cell clones cocultured in overnight assays with autologous LCL pre-pulsed with epitope peptide or DMSO solvent and either tested alone (no antibody; No Ab), or in the presence of blocking antibodies against HLA-DP, HLA-DQ or HLA-DR (b), autologous LCL and allogeneic LCLs with HLAII types partially matched to the autologous LCL, either pre-pulsed with 5μM 20mer epitope peptide or DMSO solvent (Neg) (c) or autologous LCL either pre-pulsed with epitope

DMSO solvent (Neg), peptide or 1ng/ml S tetrameric protein (d). (a-d) Results show mean IFNγ release ±1SD and are representative of 3 experiments.

Figure 3. Cross-recognition of SARS-CoV-2 spike-specific CD4$^+$ T cell clones with human β-coronaviruses. (a) Dendrogram showing the evolutionary relationship and percentage aa similarity of SARS-CoV-2 S protein with S proteins from all known HCoVs. (b) Correlogram of the percentage aa similarities between the S1 and S2 regions of the β-HCoVs. (c, d) ELISA assays for the production of IFN-γ from CD4$^+$ T cell clones cocultured with autologous LCL pre-exposed to DMSO solvent (Neg) and epitope peptide and S1 (c), or S2 peptide mixes from human β-CoVs (15aa overlapping by 11aa) in overnight assays (d). Results show mean IFN-γ release ±1SD and are representative of 3 independent experiments. Alignments show the aa sequences of SARS-CoV-2 S CD4$^+$ T cell epitopes and the corresponding β-HCoV sequences. Amino acids highlighted in yellow are conserved with SARS-CoV-2.

Figure 4. The impact of mutations in SARS-CoV-2 VOCs on spike-specific CD4$^+$ T cell clone recognition. Representative ELISA assays for the production of IFN-γ from CD4$^+$ T cell clones cocultured with autologous LCLs loaded with purified SARS-CoV-2 WT S peptides or corresponding mutated peptides from VOCs at 10^{-5} to 10^{-11}M in overnight assays. Results show mean IFN-γ release ±1SD and are representative of 3 independent experiments.

Figure 5. The impact of mutations in SARS-CoV-2 VOCs on ex vivo CD4$^+$ T cell recognition. (a) Flow cytometry analysis of total CD4$^+$ T cells and pHLAII tetramer$^+$ (pHLAII Tet$^+$) cells in PBMCs stained with the indicated pHLAII Tet and antibodies against 21 defined TCR Vb segments. (b) Elispot assays for the production of IFN-γ in CD8$^-$PBMCs plated at 4x10^5 cells/well and incubated with purified

SARS-CoV-2 WT S peptides or corresponding mutated peptides from VOCs at 10^{-6} to 10^{-8}M. Results are shown as mean spot forming cells (SFC) ±1SD per 10^6 CD8-depleted PBMCs.

REFERENCES

1. Rydyznski Moderbacher C, Ramirez SI, Dan JM, Grifoni A, Hastie KM, Weiskopf D, Belanger S, Abbott RK, Kim C, Choi J, Kato Y, Crotty EG, Kim C, Rawlings SA, Mateus J, Tse LPV, Frazier A, Baric R, Peters B, Greenbaum J, Ollmann Saphire E, Smith DM, Sette A, Crotty S. 2020. Antigen-Specific Adaptive Immunity to SARS-CoV-2 in Acute COVID-19 and Associations with Age and Disease Severity. *Cell* 183: 996-1012 e19
2. Bonifacius A, Tischer-Zimmermann S, Dragon AC, Gussarow D, Vogel A, Krettek U, Godecke N, Yilmaz M, Kraft ARM, Hoeper MM, Pink I, Schmidt JJ, Li Y, Welte T, Maecker-Kolhoff B, Martens J, Berger MM, Lobenwein C, Stankov MV, Cornberg M, David S, Behrens GMN, Witzke O, Blasczyk R, Eiz-Vesper B. 2021. COVID-19 immune signatures reveal stable antiviral T cell function despite declining humoral responses. *Immunity* 54: 340-54 e6
3. Tregoning JS, Flight KE, Higham SL, Wang Z, Pierce BF. 2021. Progress of the COVID-19 vaccine effort: viruses, vaccines and variants versus efficacy, effectiveness and escape. *Nat Rev Immunol* 21: 626-36
4. Zuo J, Dowell AC, Pearce H, Verma K, Long HM, Begum J, Aiano F, Amin-Chowdhury Z, Hoschler K, Brooks T, Taylor S, Hewson J, Hallis B, Stapley L, Borrow R, Linley E, Ahmad S, Parker B, Horsley A, Amirthalingam G, Brown K, Ramsay ME, Ladhani S, Moss P. 2021. Robust SARS-CoV-2-specific T cell immunity is maintained at 6 months following primary infection. *Nat Immunol* 22: 620-6
5. Jung JH, Rha MS, Sa M, Choi HK, Jeon JH, Seok H, Park DW, Park SH, Jeong HW, Choi WS, Shin EC. 2021. SARS-CoV-2-specific T cell memory is sustained in COVID-19 convalescent patients for 10 months with successful development of stem cell-like memory T cells. *Nat Commun* 12: 4043
6. Moss P. 2022. The T cell immune response against SARS-CoV-2. *Nat Immunol* 23: 186-93
7. Bertoletti A, Le Bert N, Qui M, Tan AT. 2021. SARS-CoV-2-specific T cells in infection and vaccination. *Cell Mol Immunol* 18: 2307-12
8. Cohen KW, Linderman SL, Moodie Z, Czartoski J, Lai L, Mantus G, Norwood C, Nyhoff LE, Edara VV, Floyd K, De Rosa SC, Ahmed H, Whaley R, Patel SN, Prigmore B, Lemos MP, Davis CW, Furth S, O'Keefe JB, Gharpure MP, Gunisetty S, Stephens K, Antia R, Zarnitsyna VI, Stephens DS, Edupuganti S, Rouphael N, Anderson EJ, Mehta AK, Wrammert J, Suthar MS, Ahmed R, McElrath MJ. 2021. Longitudinal analysis shows durable and broad immune memory after SARS-CoV-2 infection with persisting antibody responses and memory B and T cells. *Cell Rep Med* 2: 100354
9. Painter MM, Mathew D, Goel RR, Apostolidis SA, Pattekar A, Kuthuru O, Baxter AE, Herati RS, Oldridge DA, Gouma S, Hicks P, Dysinger S, Lundgreen KA, Kuri-Cervantes L, Adamski S, Hicks A, Korte S, Giles JR, Weirick ME, McAllister CM, Dougherty J, Long S, D'Andrea K, Hamilton JT, Betts MR, Bates P, Hensley SE, Grifoni A, Weiskopf D, Sette A, Greenplate AR, Wherry EJ. 2021. Rapid induction of antigen-specific CD4(+) T cells is associated with coordinated humoral and cellular immunity to SARS-CoV-2 mRNA vaccination. *Immunity* 54: 2133-42 e3
10. Ewer KJ, Barrett JR, Belij-Rammerstorfer S, Sharpe H, Makinson R, Morter R, Flaxman A, Wright D, Bellamy D, Bittaye M, Dold C, Provine NM, Aboagye J, Fowler J, Silk SE, Alderson J, Aley PK, Angus B, Berrie E, Bibi S, Cicconi P, Clutterbuck EA, Chelysheva I, Folegatti PM, Fuskova M, Green CM, Jenkin D, Kerridge S, Lawrie A, Minassian AM, Moore M, Mujadidi Y, Plested E, Poulton I, Ramasamy MN, Robinson H, Song R, Snape MD, Tarrant R, Voysey M, Watson MEE, Douglas AD, Hill AVS, Gilbert SC, Pollard AJ, Lambe T, Oxford CVTG. 2021. T cell and antibody responses induced by a single dose of ChAdOx1 nCoV-19 (AZD1222) vaccine in a phase 1/2 clinical trial. *Nat Med* 27: 270-8
11. Tarke A, Sidney J, Kidd CK, Dan JM, Ramirez SI, Yu ED, Mateus J, da Silva Antunes R, Moore E, Rubiro P, Methot N, Phillips E, Mallal S, Frazier A, Rawlings SA, Greenbaum JA, Peters B,

Smith DM, Crotty S, Weiskopf D, Grifoni A, Sette A. 2021. Comprehensive analysis of T cell immunodominance and immunoprevalence of SARS-CoV-2 epitopes in COVID-19 cases. *Cell Rep Med* 2: 100204

12. Verhagen J, van der Meijden ED, Lang V, Kremer AE, Volkl S, Mackensen A, Aigner M, Kremer AN. 2021. Human CD4(+) T cells specific for dominant epitopes of SARS-CoV-2 Spike and Nucleocapsid proteins with therapeutic potential. *Clin Exp Immunol* 205: 363-78
13. Johansson AM, Malhotra U, Kim YG, Gomez R, Krist MP, Wald A, Koelle DM, Kwok WW. 2021. Cross-reactive and mono-reactive SARS-CoV-2 CD4+ T cells in prepandemic and COVID-19 convalescent individuals. *PLoS Pathog* 17: e1010203
14. Low JS, Vaqueirinho D, Mele F, Foglierini M, Jerak J, Perotti M, Jarrossay D, Jovic S, Perez L, Cacciatore R, Terrot T, Pellanda AF, Biggiogero M, Garzoni C, Ferrari P, Ceschi A, Lanzavecchia A, Sallusto F, Cassotta A. 2021. Clonal analysis of immunodominance and cross-reactivity of the CD4 T cell response to SARS-CoV-2. *Science* 372: 1336-41
15. Mateus J, Grifoni A, Tarke A, Sidney J, Ramirez SI, Dan JM, Burger ZC, Rawlings SA, Smith DM, Phillips E, Mallal S, Lammers M, Rubiro P, Quiambao L, Sutherland A, Yu ED, da Silva Antunes R, Greenbaum J, Frazier A, Markmann AJ, Premkumar L, de Silva A, Peters B, Crotty S, Sette A, Weiskopf D. 2020. Selective and cross-reactive SARS-CoV-2 T cell epitopes in unexposed humans. *Science* 370: 89-94
16. Le Bert N, Tan AT, Kunasegaran K, Tham CYL, Hafezi M, Chia A, Chng MHY, Lin M, Tan N, Linster M, Chia WN, Chen MI, Wang LF, Ooi EE, Kalimuddin S, Tambyah PA, Low JG, Tan YJ, Bertoletti A. 2020. SARS-CoV-2-specific T cell immunity in cases of COVID-19 and SARS, and uninfected controls. *Nature* 584: 457-62
17. Braun J, Loyal L, Frentsch M, Wendisch D, Georg P, Kurth F, Hippenstiel S, Dingeldey M, Kruse B, Fauchere F, Baysal E, Mangold M, Henze L, Lauster R, Mall MA, Beyer K, Rohmel J, Voigt S, Schmitz J, Miltenyi S, Demuth I, Muller MA, Hocke A, Witzenrath M, Suttorp N, Kern F, Reimer U, Wenschuh H, Drosten C, Corman VM, Giesecke-Thiel C, Sander LE, Thiel A. 2020. SARS-CoV-2-reactive T cells in healthy donors and patients with COVID-19. *Nature* 587: 270-4
18. Loyal L, Braun J, Henze L, Kruse B, Dingeldey M, Reimer U, Kern F, Schwarz T, Mangold M, Unger C, Dorfler F, Kadler S, Rosowski J, Gurcan K, Uyar-Aydin Z, Frentsch M, Kurth F, Schnatbaum K, Eckey M, Hippenstiel S, Hocke A, Muller MA, Sawitzki B, Miltenyi S, Paul F, Mall MA, Wenschuh H, Voigt S, Drosten C, Lauster R, Lachman N, Sander LE, Corman VM, Rohmel J, Meyer-Arndt L, Thiel A, Giesecke-Thiel C. 2021. Cross-reactive CD4(+) T cells enhance SARS-CoV-2 immune responses upon infection and vaccination. *Science* 374: eabh1823
19. Harvey WT, Carabelli AM, Jackson B, Gupta RK, Thomson EC, Harrison EM, Ludden C, Reeve R, Rambaut A, Consortium C-GU, Peacock SJ, Robertson DL. 2021. SARS-CoV-2 variants, spike mutations and immune escape. *Nat Rev Microbiol* 19: 409-24
20. Greaney AJ, Starr TN, Gilchuk P, Zost SJ, Binshtein E, Loes AN, Hilton SK, Huddleston J, Eguia R, Crawford KHD, Dingens AS, Nargi RS, Sutton RE, Suryadevara N, Rothlauf PW, Liu Z, Whelan SPJ, Carnahan RH, Crowe JE, Jr., Bloom JD. 2021. Complete Mapping of Mutations to the SARS-CoV-2 Spike Receptor-Binding Domain that Escape Antibody Recognition. *Cell Host Microbe* 29: 44-57 e9
21. Cele S, Jackson L, Khoury DS, Khan K, Moyo-Gwete T, Tegally H, San JE, Cromer D, Scheepers C, Amoako DG, Karim F, Bernstein M, Lustig G, Archary D, Smith M, Ganga Y, Jule Z, Reedoy K, Hwa SH, Giandhari J, Blackburn JM, Gosnell BI, Abdool Karim SS, Hanekom W, Ngs SA, Team C-K, von Gottberg A, Bhiman JN, Lessells RJ, Moosa MS, Davenport MP, de Oliveira T, Moore PL, Sigal A. 2022. Omicron extensively but incompletely escapes Pfizer BNT162b2 neutralization. *Nature* 602: 654-6
22. GeurtsvanKessel CH, Geers D, Schmitz KS, Mykytyn AZ, Lamers MM, Bogers S, Scherbeijn S, Gommers L, Sablerolles RSG, Nieuwkoop NN, Rijsbergen LC, van Dijk LLA, de Wilde J, Alblas

K, Breugem TI, Rijnders BJA, de Jager H, Weiskopf D, van der Kuy PHM, Sette A, Koopmans MPG, Grifoni A, Haagmans BL, de Vries RD. 2022. Divergent SARS CoV-2 Omicron-reactive T- and B cell responses in COVID-19 vaccine recipients. *Sci Immunol*: eabo2202

23. Geers D, Shamier MC, Bogers S, den Hartog G, Gommers L, Nieuwkoop NN, Schmitz KS, Rijsbergen LC, van Osch JAT, Dijkhuizen E, Smits G, Comvalius A, van Mourik D, Caniels TG, van Gils MJ, Sanders RW, Oude Munnink BB, Molenkamp R, de Jager HJ, Haagmans BL, de Swart RL, Koopmans MPG, van Binnendijk RS, de Vries RD, GeurtsvanKessel CH. 2021. SARS-CoV-2 variants of concern partially escape humoral but not T-cell responses in COVID-19 convalescent donors and vaccinees. *Sci Immunol* 6
24. Gruell H, Vanshylla K, Tober-Lau P, Hillus D, Schommers P, Lehmann C, Kurth F, Sander LE, Klein F. 2022. mRNA booster immunization elicits potent neutralizing serum activity against the SARS-CoV-2 Omicron variant. *Nat Med*
25. Nelde A, Bilich T, Heitmann JS, Maringer Y, Salih HR, Roerden M, Lubke M, Bauer J, Rieth J, Wacker M, Peter A, Horber S, Traenkle B, Kaiser PD, Rothbauer U, Becker M, Junker D, Krause G, Strengert M, Schneiderhan-Marra N, Templin MF, Joos TO, Kowalewski DJ, Stos-Zweifel V, Fehr M, Rabsteyn A, Mirakaj V, Karbach J, Jager E, Graf M, Gruber LC, Rachfalski D, Preuss B, Hagelstein I, Marklin M, Bakchoul T, Gouttefangeas C, Kohlbacher O, Klein R, Stevanovic S, Rammensee HG, Walz JS. 2021. SARS-CoV-2-derived peptides define heterologous and COVID-19-induced T cell recognition. *Nat Immunol* 22: 74-85
26. Wolter N, Jassat W, Walaza S, Welch R, Moultrie H, Groome M, Amoako DG, Everatt J, Bhiman JN, Scheepers C, Tebeila N, Chiwandire N, du Plessis M, Govender N, Ismail A, Glass A, Mlisana K, Stevens W, Treurnicht FK, Makatini Z, Hsiao NY, Parboosing R, Wadula J, Hussey H, Davies MA, Boulle A, von Gottberg A, Cohen C. 2022. Early assessment of the clinical severity of the SARS-CoV-2 omicron variant in South Africa: a data linkage study. *Lancet* 399: 437-46
27. Tarke A, Sidney J, Methot N, Yu ED, Zhang Y, Dan JM, Goodwin B, Rubiro P, Sutherland A, Wang E, Frazier A, Ramirez SI, Rawlings SA, Smith DM, da Silva Antunes R, Peters B, Scheuermann RH, Weiskopf D, Crotty S, Grifoni A, Sette A. 2021. Impact of SARS-CoV-2 variants on the total CD4(+) and CD8(+) T cell reactivity in infected or vaccinated individuals. *Cell Rep Med* 2: 100355
28. Keeton R, Richardson SI, Moyo-Gwete T, Hermanus T, Tincho MB, Benede N, Manamela NP, Baguma R, Makhado Z, Ngomti A, Motlou T, Mennen M, Chinhoyi L, Skelem S, Maboreke H, Doolabh D, Iranzadeh A, Otter AD, Brooks T, Noursadeghi M, Moon JC, Grifoni A, Weiskopf D, Sette A, Blackburn J, Hsiao NY, Williamson C, Riou C, Goga A, Garrett N, Bekker LG, Gray G, Ntusi NAB, Moore PL, Burgers WA. 2021. Prior infection with SARS-CoV-2 boosts and broadens Ad26.COV2.S immunogenicity in a variant-dependent manner. *Cell Host Microbe* 29: 1611-9 e5
29. Goel RR, Painter MM, Apostolidis SA, Mathew D, Meng W, Rosenfeld AM, Lundgreen KA, Reynaldi A, Khoury DS, Pattekar A, Gouma S, Kuri-Cervantes L, Hicks P, Dysinger S, Hicks A, Sharma H, Herring S, Korte S, Baxter AE, Oldridge DA, Giles JR, Weirick ME, McAllister CM, Awofolaju M, Tanenbaum N, Drapeau EM, Dougherty J, Long S, D'Andrea K, Hamilton JT, McLaughlin M, Williams JC, Adamski S, Kuthuru O, dagger UPCPU, Frank I, Betts MR, Vella LA, Grifoni A, Weiskopf D, Sette A, Hensley SE, Davenport MP, Bates P, Luning Prak ET, Greenplate AR, Wherry EJ. 2021. mRNA vaccines induce durable immune memory to SARS-CoV-2 and variants of concern. *Science* 374: abm0829
30. Gao Y, Cai C, Grifoni A, Muller TR, Niessl J, Olofsson A, Humbert M, Hansson L, Osterborg A, Bergman P, Chen P, Olsson A, Sandberg JK, Weiskopf D, Price DA, Ljunggren HG, Karlsson AC, Sette A, Aleman S, Buggert M. 2022. Ancestral SARS-CoV-2-specific T cells cross-recognize the Omicron variant. *Nat Med*
31. Tarke A, Coelho CH, Zhang Z, Dan JM, Yu ED, Methot N, Bloom NI, Goodwin B, Phillips E, Mallal S, Sidney J, Filaci G, Weiskopf D, da Silva Antunes R, Crotty S, Grifoni A, Sette A. 2022.

SARS-CoV-2 vaccination induces immunological T cell memory able to cross-recognize variants from Alpha to Omicron. *Cell*

32. de Silva TI, Liu G, Lindsey BB, Dong D, Moore SC, Hsu NS, Shah D, Wellington D, Mentzer AJ, Angyal A, Brown R, Parker MD, Ying Z, Yao X, Turtle L, Dunachie S, Consortium C-GU, Maini MK, Ogg G, Knight JC, Investigators IC, Peng Y, Rowland-Jones SL, Dong T. 2021. The impact of viral mutations on recognition by SARS-CoV-2 specific T cells. *iScience* 24: 103353
33. Rudolph MG, Stanfield RL, Wilson IA. 2006. How TCRs bind MHCs, peptides, and coreceptors. *Annu Rev Immunol* 24: 419-66
34. Draenert R, Altfeld M, Brander C, Basgoz N, Corcoran C, Wurcel AG, Stone DR, Kalams SA, Trocha A, Addo MM, Goulder PJ, Walker BD. 2003. Comparison of overlapping peptide sets for detection of antiviral CD8 and CD4 T cell responses. *J Immunol Methods* 275: 19-29
35. Long HM, Haigh TA, Gudgeon NH, Leen AM, Tsang CW, Brooks J, Landais E, Houssaint E, Lee SP, Rickinson AB, Taylor GS. 2005. CD4+ T-cell responses to Epstein-Barr virus (EBV) latent-cycle antigens and the recognition of EBV-transformed lymphoblastoid cell lines. *J Virol* 79: 4896-907
36. Crompton L, Khan N, Khanna R, Nayak L, Moss PA. 2008. CD4+ T cells specific for glycoprotein B from cytomegalovirus exhibit extreme conservation of T-cell receptor usage between different individuals. *Blood* 111: 2053-61
37. Cassotta A, Paparoditis P, Geiger R, Mettu RR, Landry SJ, Donati A, Benevento M, Foglierini M, Lewis DJM, Lanzavecchia A, Sallusto F. 2020. Deciphering and predicting CD4+ T cell immunodominance of influenza virus hemagglutinin. *J Exp Med* 217
38. Cueno ME, Imai K. 2020. Structural Comparison of the SARS CoV 2 Spike Protein Relative to Other Human-Infecting Coronaviruses. *Front Med (Lausanne)* 7: 594439
39. Holland CJ, Cole DK, Godkin A. 2013. Re-Directing CD4(+) T Cell Responses with the Flanking Residues of MHC Class II-Bound Peptides: The Core is Not Enough. *Front Immunol* 4: 172
40. Meckiff BJ, Ladell K, McLaren JE, Ryan GB, Leese AM, James EA, Price DA, Long HM. 2019. Primary EBV Infection Induces an Acute Wave of Activated Antigen-Specific Cytotoxic CD4(+) T Cells. *J Immunol* 203: 1276-87
41. Wei S, Charmley P, Robinson MA, Concannon P. 1994. The extent of the human germline T-cell receptor V beta gene segment repertoire. *Immunogenetics* 40: 27-36
42. Poluektov Y, George M, Daftarian P, Delcommenne MC. 2021. Assessment of SARS-CoV-2 specific CD4(+) and CD8 (+) T cell responses using MHC class I and II tetramers. *Vaccine* 39: 2110-6
43. Peng Y, Mentzer AJ, Liu G, Yao X, Yin Z, Dong D, Dejnirattisai W, Rostron T, Supasa P, Liu C, Lopez-Camacho C, Slon-Campos J, Zhao Y, Stuart DI, Paesen GC, Grimes JM, Antson AA, Bayfield OW, Hawkins D, Ker DS, Wang B, Turtle L, Subramaniam K, Thomson P, Zhang P, Dold C, Ratcliff J, Simmonds P, de Silva T, Sopp P, Wellington D, Rajapaksa U, Chen YL, Salio M, Napolitani G, Paes W, Borrow P, Kessler BM, Fry JW, Schwabe NF, Semple MG, Baillie JK, Moore SC, Openshaw PJM, Ansari MA, Dunachie S, Barnes E, Frater J, Kerr G, Goulder P, Lockett T, Levin R, Zhang Y, Jing R, Ho LP, Oxford Immunology Network Covid-19 Response TcC, Investigators IC, Cornall RJ, Conlon CP, Klenerman P, Screaton GR, Mongkolsapaya J, McMichael A, Knight JC, Ogg G, Dong T. 2020. Broad and strong memory CD4(+) and CD8(+) T cells induced by SARS-CoV-2 in UK convalescent individuals following COVID-19. *Nat Immunol* 21: 1336-45
44. Gonzalez-Galarza FF, McCabe A, Santos E, Jones J, Takeshita L, Ortega-Rivera ND, Cid-Pavon GMD, Ramsbottom K, Ghattaoraya G, Alfirevic A, Middleton D, Jones AR. 2020. Allele frequency net database (AFND) 2020 update: gold-standard data classification, open access genotype data and new query tools. *Nucleic Acids Res* 48: D783-D8
45. Taylor GS, Long HM, Brooks JM, Rickinson AB, Hislop AD. 2015. The immunology of Epstein-Barr virus-induced disease. *Annu Rev Immunol* 33: 787-821

46. Peng Y, Felce SL, Dong D, Penkava F, Mentzer AJ, Yao X, Liu G, Yin Z, Chen JL, Lu Y, Wellington D, Wing PAC, Dominey-Foy DCC, Jin C, Wang W, Hamid MA, Fernandes RA, Wang B, Fries A, Zhuang X, Ashley N, Rostron T, Waugh C, Sopp P, Hublitz P, Beveridge R, Tan TK, Dold C, Kwok AJ, Rich-Griffin C, Dejnirattisa W, Liu C, Kurupati P, Nassiri I, Watson RA, Tong O, Taylor CA, Kumar Sharma P, Sun B, Curion F, Revale S, Garner LC, Jansen K, Ferreira RC, Attar M, Fry JW, Russell RA, Consortium C, Stauss HJ, James W, Townsend A, Ho LP, Klenerman P, Mongkolsapaya J, Screaton GR, Dendrou C, Sansom SN, Bashford-Rogers R, Chain B, Smith GL, McKeating JA, Fairfax BP, Bowness P, McMichael AJ, Ogg G, Knight JC, Dong T. 2022. An immunodominant NP105-113-B*07:02 cytotoxic T cell response controls viral replication and is associated with less severe COVID-19 disease. *Nat Immunol* 23: 50-61
47. Dykema AG, Zhang B, Woldemeskel BA, Garliss CC, Cheung LS, Choudhury D, Zhang J, Aparicio L, Bom S, Rashid R, Caushi JX, Hsiue EH, Cascino K, Thompson EA, Kwaa AK, Singh D, Thapa S, Ordonez AA, Pekosz A, D'Alessio FR, Powell JD, Yegnasubramanian S, Zhou S, Pardoll DM, Ji H, Cox AL, Blankson JN, Smith KN. 2021. Functional characterization of CD4+ T cell receptors crossreactive for SARS-CoV-2 and endemic coronaviruses. *J Clin Invest* 131
48. Swadling L, Diniz MO, Schmidt NM, Amin OE, Chandran A, Shaw E, Pade C, Gibbons JM, Le Bert N, Tan AT, Jeffery-Smith A, Tan CCS, Tham CYL, Kucykowicz S, Aidoo-Micah G, Rosenheim J, Davies J, Johnson M, Jensen MP, Joy G, McCoy LE, Valdes AM, Chain BM, Goldblatt D, Altmann DM, Boyton RJ, Manisty C, Treibel TA, Moon JC, Investigators CO, van Dorp L, Balloux F, McKnight A, Noursadeghi M, Bertoletti A, Maini MK. 2022. Pre-existing polymerase-specific T cells expand in abortive seronegative SARS-CoV-2. *Nature* 601: 110-7
49. Phillips RE, Harcourt GC, Price DA. 2001. CD4+ T cells: The great escape. *Nat Med* 7: 777-8
50. Naranbhai V, Nathan A, Kaseke C, Berrios C, Khatri A, Choi S, Getz MA, Tano-Menka R, Ofoman O, Gayton A, Senjobe F, Zhao Z, St Denis KJ, Lam EC, Carrington M, Garcia-Beltran WF, Balazs AB, Walker BD, Iafrate AJ, Gaiha GD. 2022. T cell reactivity to the SARS-CoV-2 Omicron variant is preserved in most but not all individuals. *Cell*

METHODS

Donor characteristics and ethical statement

The study was approved by the North West – Preston Research Ethics Committee, UK (20/NW/0240) and all participants gave written informed consent and received no compensation. Blood was collected in June-September from 20 healthcare workers (HCW), 10 males and 10 females aged 28-64, 3-6 months post infection during the first wave of SARS-CoV-2 WT (D614G) infection in the UK. Control samples were collected from SARS-CoV-2 uninfected healthy (UH) individuals (n=14; 6 males and 8 females aged 24-63) confirmed to be seronegative for SARS-CoV-2 (Fig. S1), or collected prior to the pandemic from healthy donors as part of an ethically approved study (South Birmingham Research Ethics Committee 14/WM/1254). Subsequent samples were collected from those UH individuals who remained uninfected following vaccination with Pfizer BioNtech BNT162b2 or Astrazeneca ChAdOx-1 (n=9; 3 males and 6 females aged 39-63) 1-5 months after vaccination.

Sample Preparation

Plasma and PBMCs were isolated from heparinised blood using standard Ficoll-Hypaque centrifugation. The resulting PBMC layer was washed twice with RPMI and either used directly or cryopreserved prior to use. Where stated, PBMCs were depleted of $CD8^+$ T cells ($CD8^-$PBMCs) using anti-CD8 Dynabeads (Invitrogen) to >94%, as measured by flow cytometry. Autologous Lymphoblastoid cell lines (LCLs) were generated by transformation with B95.8 EBV as previously described[51] and HLAII typing by next generation sequencing was performed at the Anthony Nolan Histocompatibility Laboratories, UK.

Synthetic peptides and protein

For stimulation of T cell responses against whole protein sequences, peptide mixes containing 15mer peptides overlapping by 11aa covering the full length of WT (D614G) SARS-CoV-2 S1 and S2 (PM-WCPV-S-2), M (PM-WCPV-VME-2) and N (PM-WCPV-NCAP-2), the S1 and S2 regions of SARS (PM-CVHSA-S-1), MERS (PM-MERS-CoV-1), HKU1 (PM-HKU1-S-1) and OC43 (PM-OC43-S-1), and control HLAII CEFX peptide mix (PM-CEFX-3) were purchased from JPT. HLAI peptide mix was generated in-house by combining 30 known EBV $CD8^+$ T cell epitope peptides[45].

For analysis of responses at the epitope level, individual 20-mer peptides overlapping by 15aa covering the full sequences of SARS-CoV-2 S, M and N were purchased from Alta Biosciences, UK. Upon epitope identification, purified epitope peptides (>85% purity) and corresponding peptides (20mers and one 15mer for which the variant 20mer peptide could not be synthesised) from SARS-CoV-2 VOCs were synthesised by Alta Biosciences, UK, and Genscript, Netherlands. All peptides were resuspended in dimethylsulphoxide (DMSO) at a concentration of 5mg/ml. The concentration of all purified epitope peptides was confirmed using a Pierce Quantitative Colorimetric Peptide assay (Thermo Scientific) that binds to the peptide amide backbone, and peptides were adjusted to equivalent concentrations. The SARS-CoV-2 S protein is a soluble prefusion stabilised form, containing proline substitutions at positions F817P, A892P, A899P, A942P, K986P, V987P[52]. Epitope sequences recognised by the isolated $CD4^+$ T cell clones are free of these stabilising mutations.

Interferon-γ Elispot assay

Whole or CD8-depleted PBMCs ($0.2\text{-}0.4x10^6$ cells) were resuspended in standard media (RPMI supplemented with 8% batch-tested FCS, 100 IU/mL penicillin and 100 μg/mL streptomycin) and added to duplicate or triplicate wells of IFNγ Elispot Pro Kit (Mabtech) plates containing 2μg/ml peptide mix, 5μg/ml purified epitope peptide or titrated concentration as stated, DMSO (negative

control) and PHA or anti-CD3 (positive controls). Samples were incubated at 37°C for 16-18hr. Plates were developed in accordance with the manufacturer's instructions and read on a Bioreader 5000 Fγ (Bio-sys GmbH). To quantify antigen-specific responses, mean DMSO values were deducted from all test wells and the results were expressed as spot forming cells (SFC) per 10^6 cells.

Polyclonal T cell generation and analysis

Polyclonal $CD4^+$ T cell lines, generated by stimulation of $CD8^-$PBMCs with 2μg/ml S, M or N peptide mix (JPT, 15aa peptides overlapping by 11aa), were cultured in RPMI supplemented with 5% batch-tested human serum (Gibco) and 50IU/ml IL-2. Following 1-4 bi-weekly repeat stimulations with the same peptide mix, 50,000 polyclonal T cells were incubated for 16-18hr in V-bottom microtest plate wells with 1ug/ml individual 20-mer peptides overlapping by 10aa covering S, M or N or DMSO (negative control). IFNγ release into the supernatant was tested by ELISA (Invitrogen) according to the manufacturer's protocol. Responses against the test peptides were considered positive if greater than twice the mean of the control wells.

T cell clone isolation and assays

$CD4^+$ T cell clones were isolated from polyclonal cultures as previously described[53]. Briefly, polyclonal $CD4^+$ T cells were selected on rechallenge with 2μg/ml appropriate peptide mix using an IFNγ cell enrichment kit (Miltenyi Biotech) followed by MACS separation using anti-PE beads. Enriched cells were cloned by limiting dilution seeding, to establish T cell clones originating from single cells. Growing microcultures were screened for reactivity against individual 20mer peptides and selected clones were expanded using standard methods[35].

$CD4^+$ T cell clones (2000 or 5000 cells per well) were incubated in V-bottom 96-well microtest plate wells with $5x10^4$ cells per well of autologous LCL or allogeneic LCLs with HLAII types partially matched to the autologous LCL. In some assays, LCLs were either pre-exposed for 1hr to 5μM 20mer epitope peptide, 2μg/ml peptide mix, or for 3hrs to 1ng/ml soluble prefusion-stabilised SARS-CoV-2 S protein[52] or equivalent volumes of DMSO (negative control) before washing and addition to the wells, or added with a titrated concentration of individual 20mer peptides. EC50 values were defined for each peptide as the concentration eliciting 50% maximum IFNγ release produced in response to the optimal WT peptide. T cell clone responses to mutated peptides from VOCs were quantified as the fold increase in concentration required to yield T cell activity equivalent to the EC50 of the WT peptide. In blocking assays, peptide-loaded or DMSO-exposed LCLs were incubated for 1hr with purified monoclonal antibodies against HLA-DR (L243, Biolegend), HLA-DQ (SPV-L3, Biotium) and HLA-DP (B7/21, Life Technologies) before addition of T cells. In all other assays, T cells were added immediately. The supernatant medium harvested after 16-18hrs was assayed for IFNγ by ELISA.

pHLAII tetramer staining and TCR Vb repertoire analysis

PBMCs from HCW-PI or uninfected healthy (UH) individuals post-vaccine were stained with optimised concentrations of peptide-HLAII tetramers (pHLAII Tet) (NIH tetramer core) containing S epitopes SSAN (DPB1*04:01/SSAN), GGNY (DPB1*02:01/GGNY) or STEC (DRB1*15:01/STEC), appropriate for the HLAII genotype of each individual. $1.5\text{-}2x10^6$ PBMCs were used per tube to enable collection of low frequency pHLAII Tet^+ events. PBMCs were washed in PBS and stained with pHLAII Tet in batch-tested human serum for 1hr at 37°C with regular resuspension. After incubation, cells were washed in PBS and stained at RT for 30mins with BV510 anti-CD14 (MΦP9), BV510 anti-CD19 (SJ25C1), LIVE/DEAD Fixable Aqua Dead Cell Stain Kit (Invitrogen), BV650 anti-CD3 (OKT3) and PerCP anti-CD4 (RPA-T4), plus appropriate combinations of the following TCR Vβ antibodies covering >70% of normal human expressed TCR Vβ repertoire[41]: FITC anti-TCR Vβ3 (CH92), FITC anti-TCR Vβ4

(WJF24), FITC anti-TCR Vβ5.1 (IMMU 157), FITC anti-TCR Vβ5.2 (36213), FITC anti-TCR Vβ8 (56C5.2), FITC anti-TCR Vβ13.1 (H131), FITC anti-TCR Vβ20 (ELL1.4), FITC anti-TCR Vβ22 (IMMU 546), APC anti-TCR Vβ1 (REA662), APC anti-TCR Vβ5.3 (REA670), APC anti-TCR Vβ7.1 (REA871), APC anti-TCR Vβ7.2 (REA677), APC anti-TCR Vβ13.6 (REA554), APC anti-TCR Vβ14 (REA557), APC anti-TCR Vβ23 (REA497), AF647 anti-TCR Vβ13.2 (H132), APC-Vio770 anti-TCR Vβ2 (REA654), APC-Vio770 anti-TCR Vβ11 (REA559), APC-Vio770 anti-TCR Vβ16 (REA553), APC-Vio770 anti-TCR Vβ17 (REA915), APC-Vio770 anti-TCR Vβ21.3 (REA894). Cells were washed and resuspended in PBS following staining and data was acquired on a BD LSR Fortessa X20 flow cytometer (BD Biosciences) using FACSDiva (Version 9.0). All data was processed using FlowJo analysis software (Version 10.6.1).

Serological analysis

Quantitative IgG antibody titres against SARS-CoV-2 S and N and HCoV family S proteins were measured using a multiplex serology assays (V-PLEX COVID-19 Coronavirus Panel 2 [IgG] kit, catalogue number K15369U), according to the manufacturer's instructions. In brief, 96-well plates were blocked and washed. Samples were pre-diluted 1:4000 in provided sample diluent and added to the wells in duplicate alongside the reference standard and assay kit controls. Following incubation, washing and addition of anti-IgG detection antibodies, read buffer was added to all wells and plates were immediately measured using a MESO Quickplex SQ 120 System (Meso Scale Discovery). Data were generated by Methodological Mind software (version 1.0.36), adjusted for sample dilutions and analysed using MSD Discovery Workbench (version 4.0).

Bioinformatic analysis

Spike amino acid alignments were performed using the MUSCLE algorithm[54] with default settings. Protein sequence identity was calculated using Expasy[55]. Correlation plots were prepared in R version 4.0.3 using corrplot (v0.84).

Statistics & reproducibility

Information on the study design is available in the Nature Research Reporting Summary linked to this article. No statistical methods were used to predetermine cohort sizes and researchers were not blinded to the serostatus of donors before Elispot and serological assays. All statistical tests were performed in GraphPad Prism (v. 9.3.1).

DATA AVAILABILITY

Data in this study are available within the article and from the corresponding author on reasonable request. Statistical source data are provided with this paper.

METHODS ONLY REFERENCES

51. Frisan T, Levitsky V, Masucci M. 2001. Generation of lymphoblastoid cell lines (LCLs). *Methods Mol Biol* 174: 125-7
52. Hsieh CL, Goldsmith JA, Schaub JM, DiVenere AM, Kuo HC, Javanmardi K, Le KC, Wrapp D, Lee AG, Liu Y, Chou CW, Byrne PO, Hjorth CK, Johnson NV, Ludes-Meyers J, Nguyen AW, Park J, Wang N, Amengor D, Lavinder JJ, Ippolito GC, Maynard JA, Finkelstein IJ, McLellan JS. 2020. Structure-based design of prefusion-stabilized SARS-CoV-2 spikes. *Science* 369: 1501-5
53. Long HM, Leese AM, Chagoury OL, Connerty SR, Quarcoopome J, Quinn LL, Shannon-Lowe C, Rickinson AB. 2011. Cytotoxic CD4+ T cell responses to EBV contrast with CD8 responses in breadth of lytic cycle antigen choice and in lytic cycle recognition. *J Immunol* 187: 92-101
54. Edgar RC. 2004. MUSCLE: multiple sequence alignment with high accuracy and high throughput. *Nucleic Acids Res* 32: 1792-7
55. Duvaud S, Gabella C, Lisacek F, Stockinger H, Ioannidis V, Durinx C. 2021. Expasy, the Swiss Bioinformatics Resource Portal, as designed by its users. *Nucleic Acids Res* 49: W216-W27

Figure 1

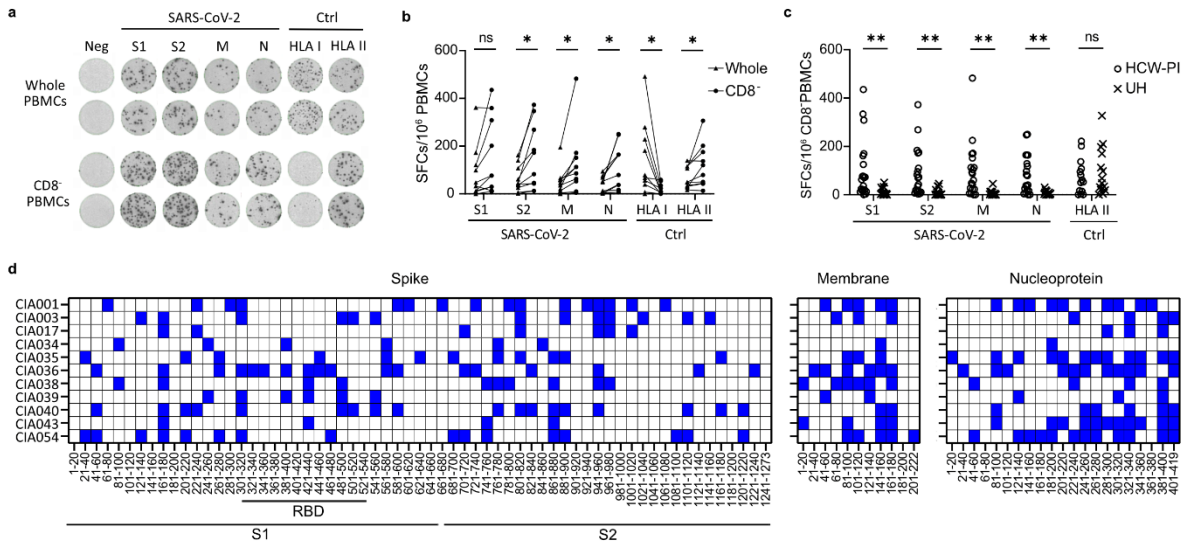
a
SARS-CoV-2
Ctrl
Neg
S1
S2
M
N
HLA I
HLA II
Whole PBMCs
CD8- PBMCs
b
SFCs/10^6 PBMCs
Whole
CD8-
ns
S1
S2
M
N
HLA I
HLA II
SARS-CoV-2
Ctrl
c
SFCs/10^6 CD8- PBMCs
HCW-PI
UH
d
Spike
Membrane
Nucleoprotein
CIA001
CIA003
CIA017
CIA034
CIA035
CIA036
CIA038
CIA039
CIA040
CIA043
CIA054
RBD
S1
S2

Figure 2

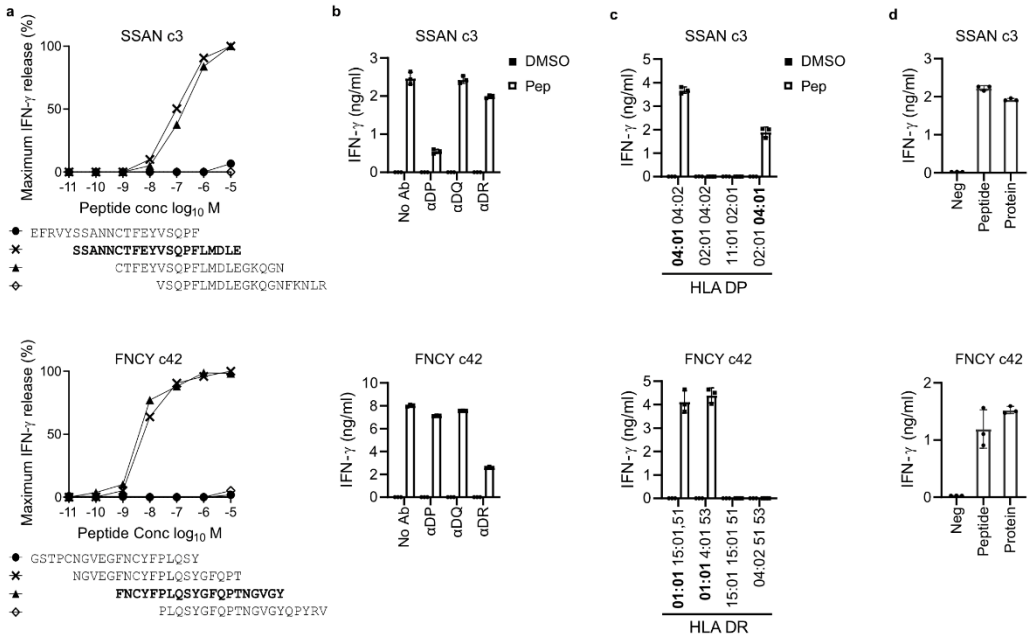
a
SSAN c3
Maximum IFN-γ release (%)
Peptide conc log10 M
EFRVYSSANNCTFEYVSQPF
SSANNCTFEYVSQPFLMDLE
CTFEYVSQPFLMDLEGKQGN
VSQPFLMDLEGKQGNFKNLR
FNCY c42
Peptide Conc log10 M
GSTPCNGVEGFNCYFPLQSY
NGVEGFNCYFPLQSYGFQPT
FNCYFPLQSYGFQPTNGVGY
PLQSYGFQPTNGVGYQPYRV
b
SSAN c3
IFN-γ (ng/ml)
DMSO
Pep
No Ab
αDP
αDQ
αDR
FNCY c42
c
SSAN c3
04:01 04:02
02:01 04:02
11:01 02:01
02:01 04:01
HLA DP
FNCY c42
01:01 15:01,51
01:01 4:01 53
15:01 15:01 51
04:02 51 53
HLA DR
d
SSAN c3
Neg
Peptide
Protein
FNCY c42

Figure 3

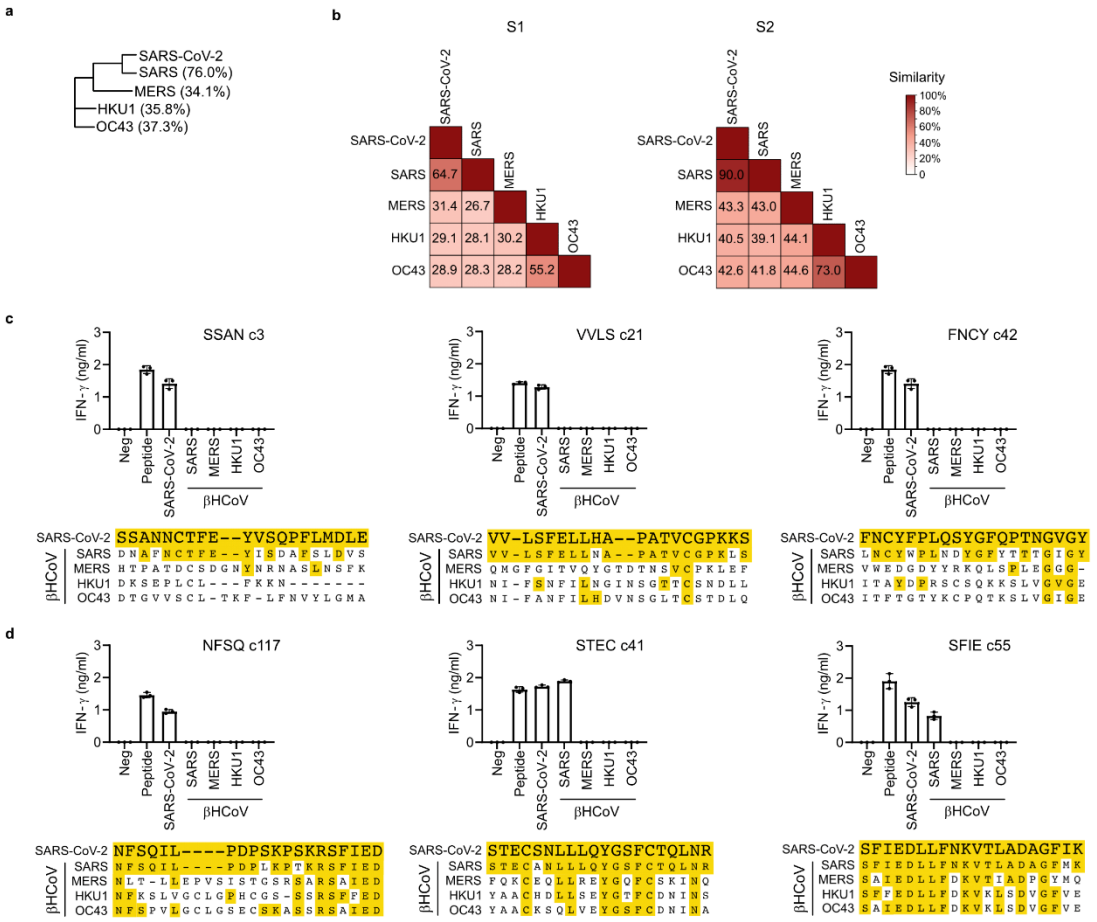
a
SARS-CoV-2
SARS (76.0%)
MERS (34.1%)
HKU1 (35.8%)
OC43 (37.3%)
b
S1
S2
Similarity
100%
80%
60%
40%
20%
0
SARS-CoV-2 64.7 31.4 29.1 28.9
SARS 26.7 28.1 28.3
MERS 30.2 28.2
HKU1 55.2
OC43
SARS-CoV-2 90.0 43.3 40.5 42.6
SARS 43.0 39.1 41.8
MERS 44.1 44.6
HKU1 73.0
OC43
c
SSAN c3
VVLS c21
FNCY c42
IFN-γ (ng/ml)
Neg
Peptide
SARS-CoV-2
SARS
MERS
HKU1
OC43
βHCoV
SARS-CoV-2 SSANNCTFE--YVSQPFLMDLE
SARS DNAFNCTFE--YISDAFSLDVS
MERS HTPATDCSDGNYNRNASLNSFK
HKU1 DKSEPLCL---FKKN-------
OC43 DTGVVSCL-TKF-LFNVYLGMA
SARS-CoV-2 VV-LSFELLHA--PATVCGPKKS
SARS VV-LSFELLNA--PATVCGPKLS
MERS QMGFGITVQYGTDTNSVCPKLEF
HKU1 NI-FSNFILNGINSGTTCSNDLL
OC43 NI-FANFILHDVNSGLTCSTDLQ
SARS-CoV-2 FNCYFPLQSYGFQPTNGVGY
SARS LNCYWPLNDYGFYTTTGIGY
MERS VWEDGDYYRKQLSPLEGGG-
HKU1 ITAYDPRSCSQKKSLVGVGE
OC43 ITFTGTYKCPQTKSLVGIGE
d
NFSQ c117
STEC c41
SFIE c55
SARS-CoV-2 NFSQIL----PDPSKPSKRSFIED
SARS NFSQIL----PDPLKPTKRSFIED
MERS NLT-LLEPVSISTGSRSARSAIED
HKU1 NFKSLVGCLGPHCGS-SSRSFFED
OC43 NFSPVLGCLGSECSKASSRSAIED
SARS-CoV-2 STECSNLLLQYGSFCTQLNR
SARS STECANLLLQYGSFCTQLNR
MERS FQKCEQLLREYGQFCSKINQ
HKU1 YAACHDLLSEYGTFCDNINS
OC43 YAACKSQLVEYGSFCDNINA
SARS-CoV-2 SFIEDLLFNKVTLADAGFIK
SARS SFIEDLLFNKVTLADAGFMK
MERS SAIEDLLFDKVTIADPGYMQ
HKU1 SFFEDLLFDKVKLSDVGFVE
OC43 SAIEDLLFDKVKLSDVGFVE

Figure 4

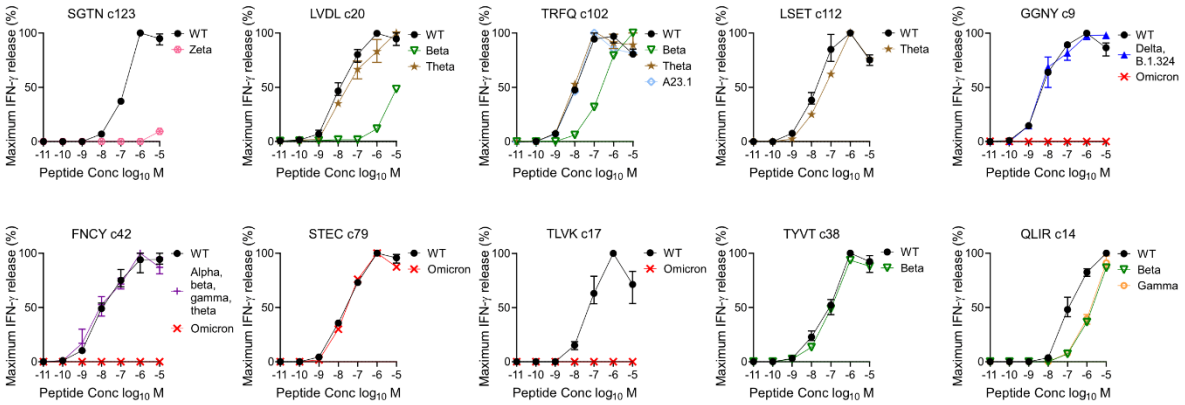
SGTN c123
WT
Zeta
LVDL c20
WT
Beta
Theta
TRFQ c102
WT
Beta
Theta
A23.1
LSET c112
WT
Theta
GGNY c9
WT
Delta, B.1.324
Omicron
FNCY c42
WT
Alpha, beta, gamma, theta
Omicron
STEC c79
WT
Omicron
TLVK c17
WT
Omicron
TYVT c38
WT
Beta
QLIR c14
WT
Beta
Gamma
Maximum IFN-γ release (%)
Peptide Conc log10 M

Figure 5

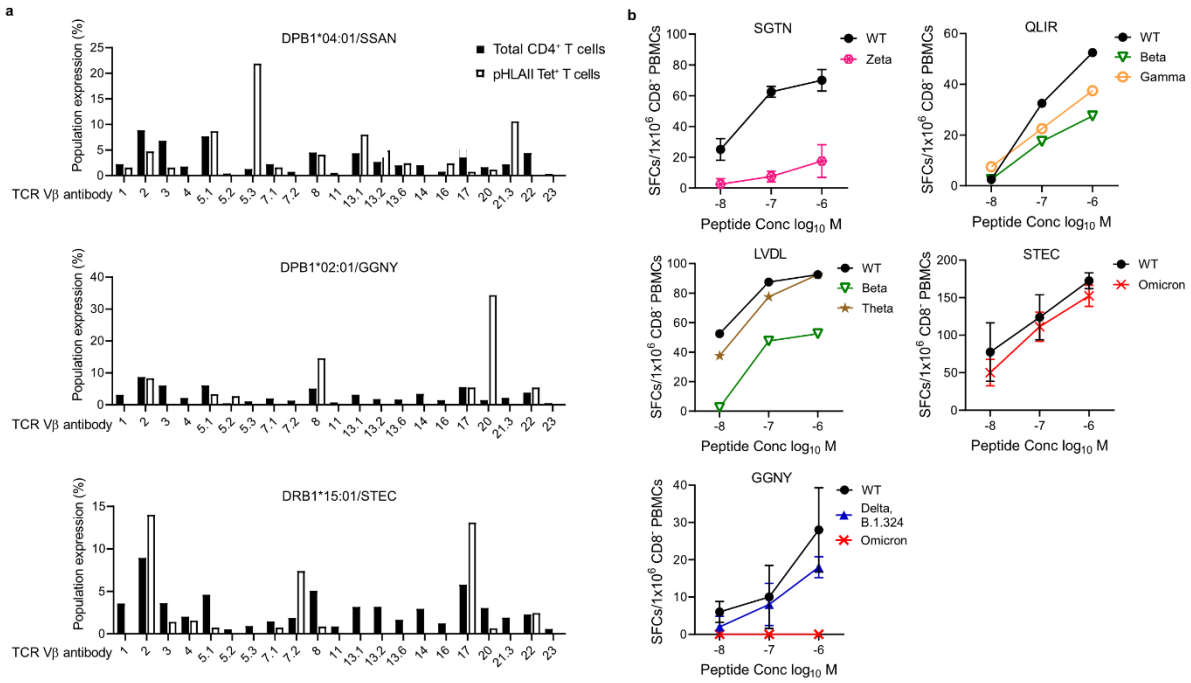
a
DPB1*04:01/SSAN
Total CD4+ T cells
pHLAII Tet+ T cells
Population expression (%)
TCR Vβ antibody
DPB1*02:01/GGNY
DRB1*15:01/STEC
b
SGTN
WT
Zeta
QLIR
WT
Beta
Gamma
LVDL
WT
Beta
Theta
STEC
WT
Omicron
GGNY
WT
Delta, B.1.324
Omicron
SFCs/1x10^6 CD8- PBMCs
Peptide Conc log10 M

Extended Data Figure 1

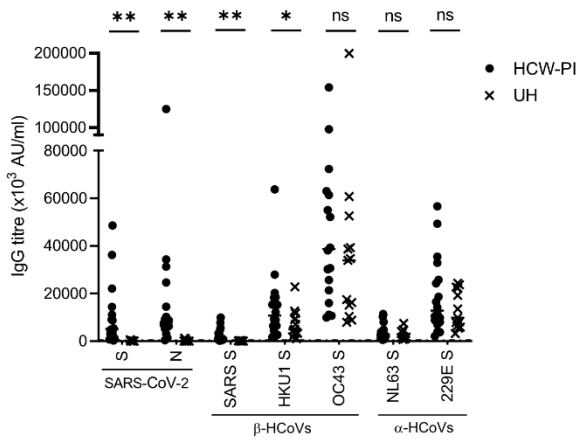

Extended Data Fig. 1. Antibody responses to coronaviruses in healthcare workers post-infection and uninfected healthy individuals. Multiplex serology assays showing IgG antibody titres against SARS-CoV-2 S and N proteins and S protein from HCoVs in HCW-PI 3-6 months post-infection (n=18) and UH individuals (n=13). Significance was determined by two-sided Mann-Whitney U test, **p<0.0001, *p=0.0379.

Extended Data Figure 2

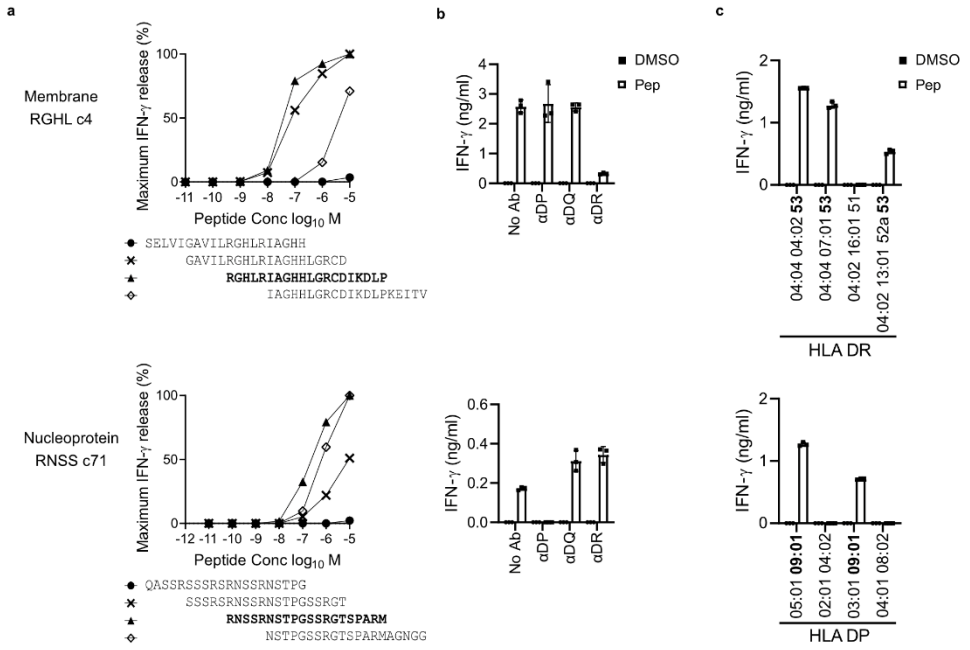

Extended Data Fig. 2. Characterisation of novel membrane and nucleoprotein CD4$^+$ T cell epitopes. ELISA assays for the production of IFNγ from CD4$^+$ T cell clones cocultured in overnight assays with (a) autologous lymphoblastoid cell line (LCL) loaded with individual 20mer peptides overlapping by 15aa (10^{-5} to 10^{-11}M), (b) autologous LCL pre-pulsed with epitope peptide or DMSO solvent and either tested alone (no antibody; No Ab), or in the presence of blocking antibodies against HLA-DP, HLA-DQ or HLA-DR, and (c) autologous LCL and allogeneic LCLs with HLAII types partially matched to the autologous LCL, either pre-pulsed with 5μM 20mer epitope peptide or DMSO solvent (neg). (a-c) Results show mean IFNγ release ±1SD and are representative of 3 experiments.

Extended Data Figure 3

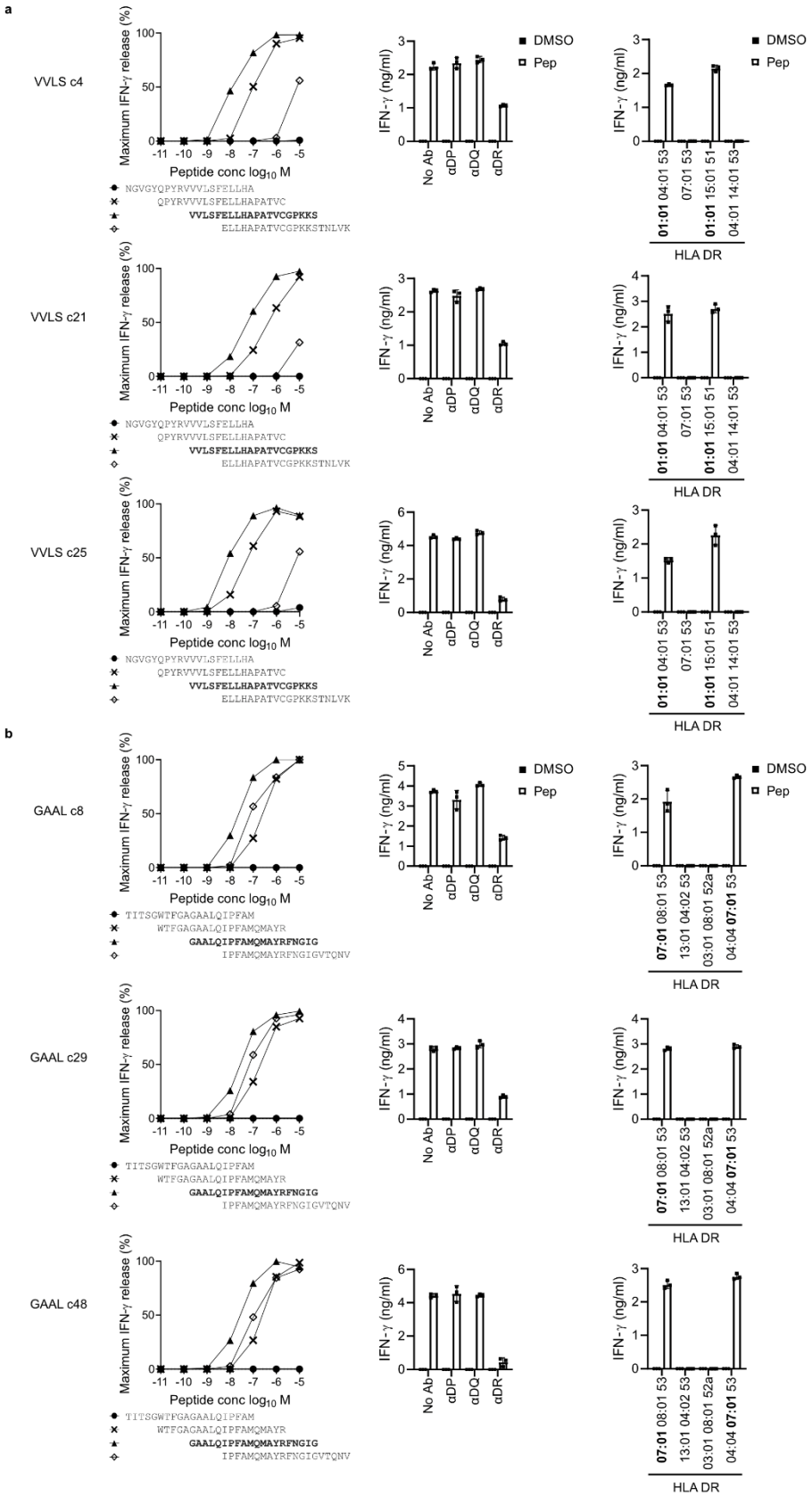

Extended Data Fig. 3. Mapping of multiple CD4$^+$ T cell clones against S epitopes. ELISA assays for the production of IFNγ from (a) three VVLS-specific and (b) three GAAL-specific CD4$^+$ T cell clones cocultured in overnight assays with autologous lymphoblastoid cell line (LCL) loaded with individual 20mer peptides overlapping by 15aa (10^{-5} to 10^{-11}M) (left panels), autologous LCL pre-pulsed with epitope peptide or DMSO solvent and either tested alone (no antibody; No Ab), or in the presence of blocking antibodies against HLA-DP, HLA-DQ or HLA-DR (middle panels) and autologous LCL and allogeneic LCLs with HLAII types partially matched to the autologous LCL, either pre-pulsed with 5μM 20mer epitope peptide or DMSO solvent (neg) (right panels). (a-c) Results show mean IFNγ release ±1SD and are representative of 3 experiments.

Extended Data Figure 4

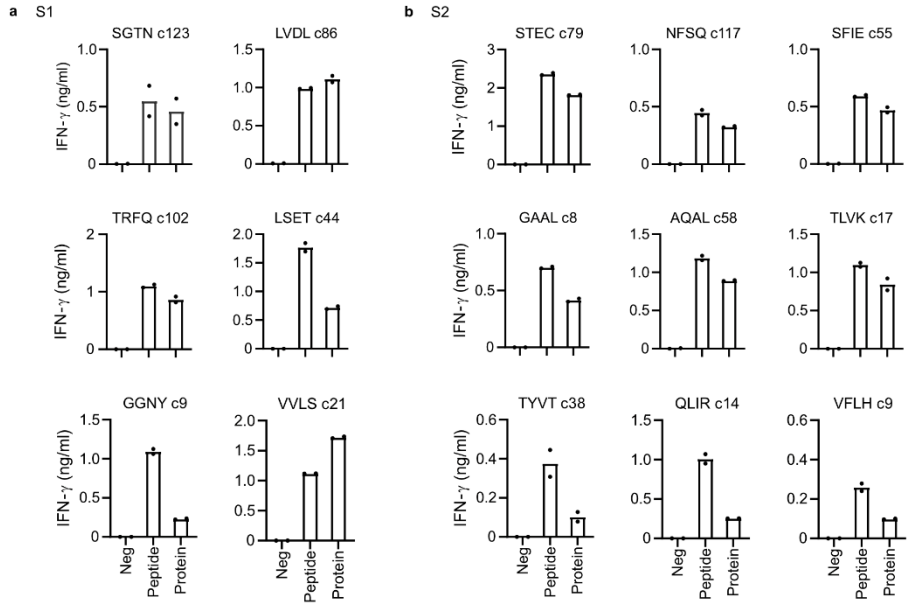

Extended Data Fig. 4. Spike-specific CD4⁺ T cell clone recognition of S protein. ELISA assays for the production of IFNγ from CD4⁺ T cell clones cocultured overnight with autologous LCL pre-pulsed with DMSO solvent (neg), epitope peptide or 1ng/ml S tetrameric protein. Data is shown for CD4⁺ T cell clones specific for the 15 S epitopes not presented in Fig. 2. Results show mean IFNγ release and are representative of 2 experiments.

Extended Data Figure 5

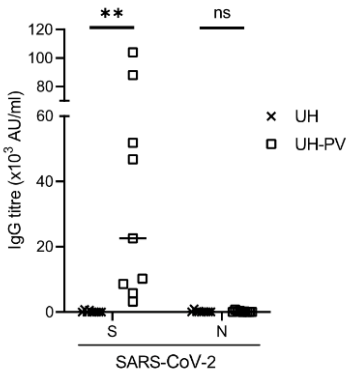

Extended Data Fig. 5. SARS-CoV-2 S and N-specific IgG antibody titres in uninfected healthy individuals pre and post-vaccination. Multiplex serology assays showing IgG antibody titres against SARS-CoV-2 S and N proteins in UH individuals (n=9) and the same UH individuals 1-5 months post SARS-CoV-2 vaccination (UH-PV). Significance was determined by two-sided Wilcoxon test **p=0.0039.

Extended Data Figure 6

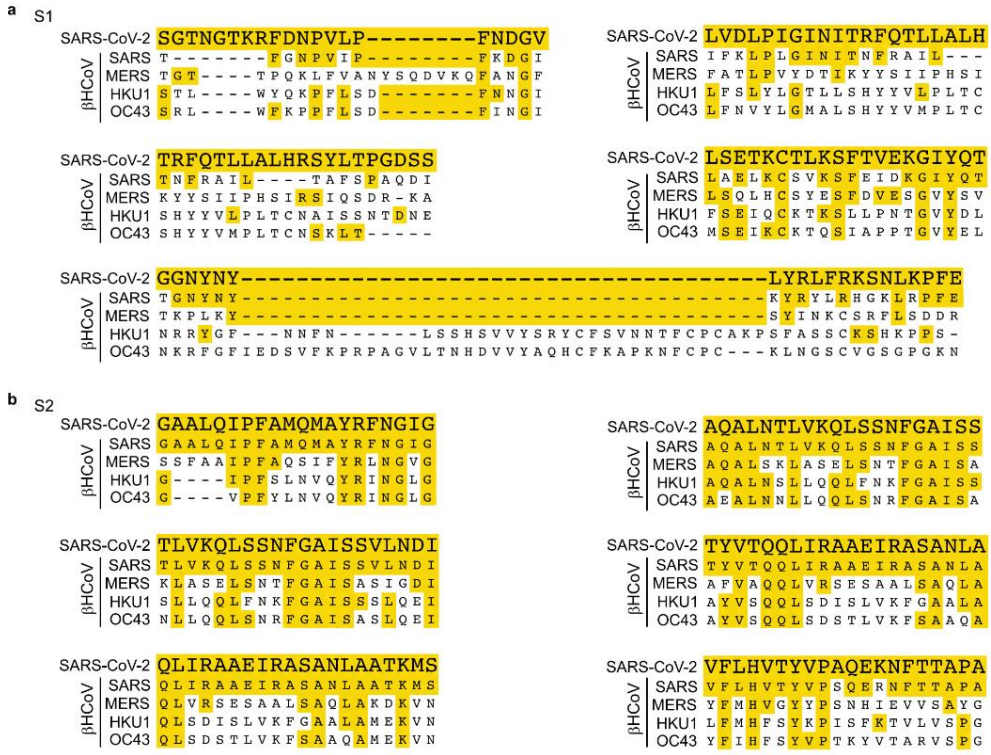

Extended Data Fig. 6. Alignment of SARS-CoV-2 spike CD4⁺ T cell epitopes with the corresponding amino acid sequences of other β–HCoVs. Alignments show the aa sequences of SARS-CoV-2 S-derived CD4⁺ T cell epitopes in (a) S1 and (b) S2 with the corresponding sequences of other β-HCoVs, for those epitopes not shown in Fig. 3. Amino acids highlighted in yellow are conserved with SARS-CoV-2.

Extended Data Figure 7

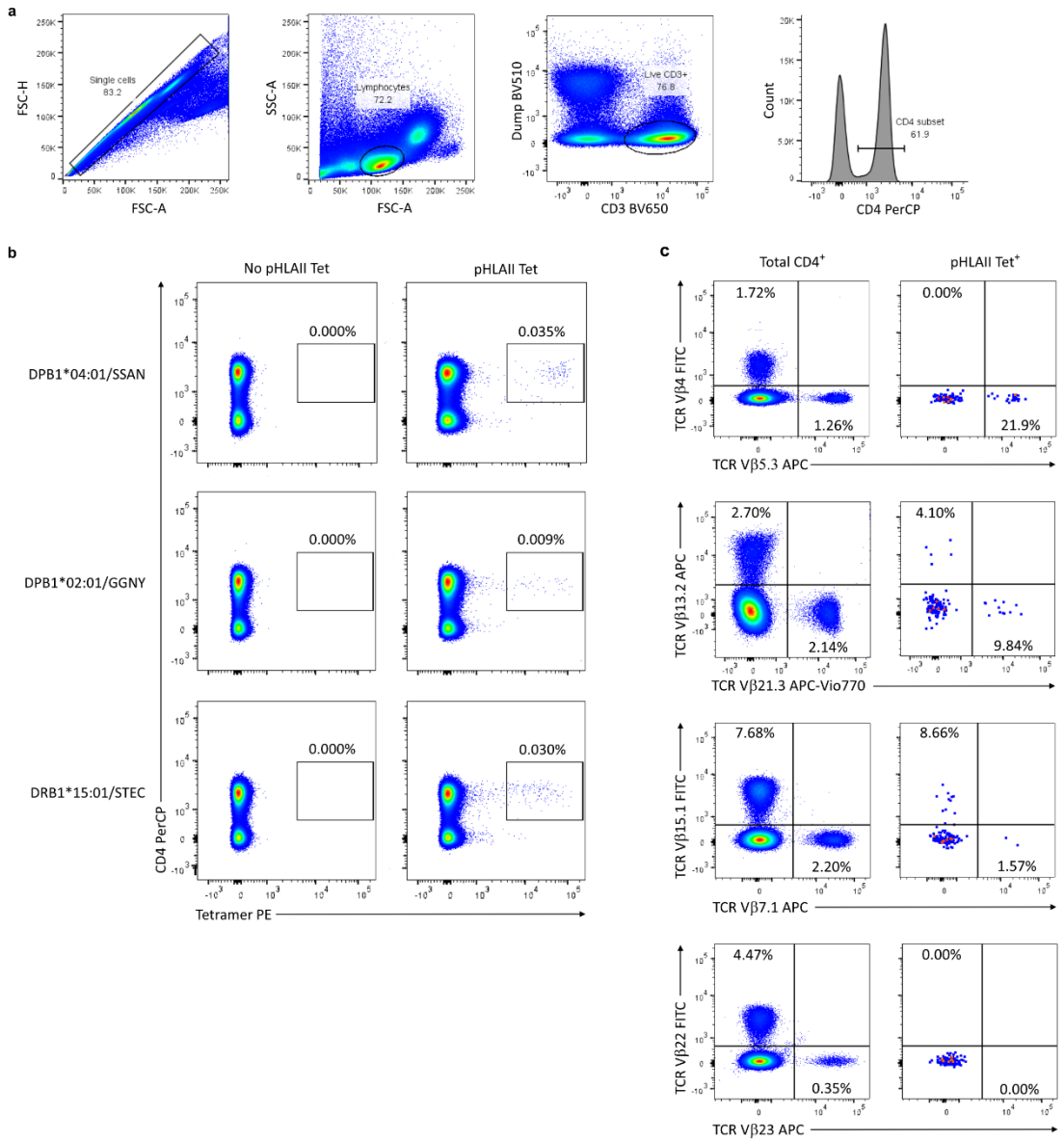

Extended Data Fig. 7. pHLAII tetramer and TCR Vβ analysis. Flow cytometry of PBMCs stained with pHLAII Tet and antibodies against defined TCR Vβ segments. (a) Gating strategy used for analysis. (b) Representative flow cytometry plots of pHLAII Tet$^+$ events within the total CD4$^+$ T cell population of PBMCs either exposed to no pHLAII Tet or DPB1*04:01/SSAN, DPB1*02:01/GGNY or DRB1*15:01/STEC pHLAII Tets. (c) Representative flow cytometry plots of individual TCR Vβ antibody staining on total CD4$^+$ T cells and pHLAII Tet$^+$ cells in PBMCs stained with the DPB1*04:01/SSAN tetramer.

Supplementary Table 1 – SARS-CoV-2 CD4+ T-cell clones isolated

Protein	aa coordinates	Epitope	Donor	Number of clones isolated
Spike	71-90	SGTNGTKRFDNPVLPFNDGV	CIA001	1
Spike	161-180	SSANNCTFEYVSQPFLMDLE	CIA038	21
Spike	226-245	LVDLPIGINITRFQTLLALH	CIA001	3
Spike	236-255	TRFQTLLALHRSYLTPGDSS	CIA001	6
Spike	296-315	LSETKCTLKSFTVEKGIYQT	CIA001	1
Spike	446-465	GGNYNYLYRLFRKSNLKPFE	CIA036	4
			CIA037	3
Spike	486-505	FNCYFPLQSYGFQPTNGVGY	CIA038	4
Spike	511-530	VVLSFELLHAPATVCGPKKS	CIA037	4
Spike	746-765	STECSNLLLQYGSFCTQLNR	CIA038	29
Spike	801-820	NFSQILPDPSKPSKRSFIED	CIA001	4
Spike	816-835	SFIEDLLFNKVTLADAGFIK	CIA035	5
Spike	891-910	GAALQIPFAMQMAYRFNGIG	CIA035	22
Spike	956-975	AQALNTLVKQLSSNFGAISS	CIA038	27
Spike	961-980	TLVKQLSSNFGAISSVLNDI	CIA001	8
Spike	1006-1025	TYVTQQLIRAAEIRASANLA	CIA001	2
Spike	1011-1030	QLIRAAEIRASANLAATKMS	CIA001	3
Spike	1061-1080	VFLHVTYVPAQEKNFTTAPA	CIA001	4
Membrane	146-165	RGHLRIAGHHLGRCDIKDLP	CIA001	3
Membrane	161-180	IKDLPKEITVATSRTLSYYK	CIA001	1
Nucleoprotein	196-215	RNSSRNSTPGSSRGTSPARM	CIA001	2
Nucleoprotein	281-300	QTQGNFGDQELIRQGTDYKH	CIA001	2